

BEHAVIOR OF REINFORCED CONCRETE WIDE BEAMS

(An Experimental Study on Wide Beams at Medium and High Reinforcement Ratios at Shear Span to Depth Ratio of 4.5)



Thesis of Master of Science

By

Muhammad Shehzad Hassan

(NUST201362246MSCEE15213F)

NUST Institute of Civil Engineering

School of Civil and Environmental Engineering

National University of Sciences and Technology

Islamabad, Pakistan

(2016)

This is to certify that
thesis entitled

BEHAVIOR OF REINFORCED CONCRETE WIDE BEAMS

Submitted by

Muhammad Shehzad Hassan

Has been accepted towards the partial fulfillment
of
the requirements
for
Master of Science in Civil Engineering

Dr. Wasim Khaliq
NUST Institute of Civil Engineering, NUST Islamabad
National University of Sciences and Technology Islamabad

BEHAVIOR OF REINFORCED CONCRETE WIDE BEAMS

By

Muhammad Shehzad Hassan

A Thesis

of

Master of Sciences

Submitted to the

NUST Institute of Civil Engineering

National University of Sciences and Technology

Islamabad

In partial fulfillment of the requirements

For the degree of

Master of Science in Civil Engineering

2016

Dedicated to
My parents, teachers and all well wishers

ACKNOWLEDGEMENT

I am grateful to Allah Almighty whose blessing gave me the strength to complete this study. I express my gratitude and sincere thanks to my advisor Dr. Rao Arsalan and co-advisor Dr Khaliq -ur- Rashid Kayani for their advice and kind supervision throughout the period of research. I am also thankful to the guidance and evaluation committee members for their guidance.

I must not forget the supporting role of my co-advisor Dr. Khaliq -ur- Rashid Kayani who sponsored this research.

I extend my gratitude to master students, Abdul Mujeeb Khan, Muhammad Waqas and Farhan, who assisted me in conducting testing of reinforced concrete wide beams.

I am also thankful to the administration and laboratory staff of the NUST Institute of Civil Engineering for their help extended in the research work.

I appreciate the support provided to me by my parents in the form of prayers.

ABSTRACT

Researchers have a concern that normal beam design procedures are not fully applicable to RC wide beams. Many studies have been conducted on RC wide beams and researchers have diverse results regarding shear strength of wide beams. Studies have shown that the shear behavior of RC wide beams varies depending on various factors such as aspect ratio (b/h), shear span to depth ratio (a'/d), longitudinal reinforcement configuration, amount and configuration of vertical stirrups, presence of temperature and shrinkage reinforcement and stirrup spacing across the width of beam.

Another important subject is the behavior of RC wide beams at high longitudinal reinforcement ratios (closer to balanced reinforcement ratio). A beam designed under balanced reinforcement conditions and secured for shear is expected to fail in a ductile manner but there is a possibility of stiffer mode of failure at high longitudinal reinforcement ratios. Such stiff mode of failure can cause a beam fail in a sudden manner. It is important to mention that wide beams may be reinforced closer to balanced reinforcement ratio to meet high flexure demands. Moreover, web shear reinforcement is provided in all practical concrete beams. Therefore, there is a need to study the behavior of RC wide beams with web shear reinforcement demanded from the ultimate load which would cause flexure failure. How the shear strength ($V_c + V_s$) at ultimate load varies with the increasing percentage of longitudinal reinforcement ratio for a shear secured beam?

Present study encompasses testing of eight full scale, simply supported RC wide beams. Beams are divided into two series being W and M. W series consists of 30 inches wide beams while M series contains 40 inches wide beams. In each series there are two different longitudinal reinforcement ratios provided. Four point bending method was adopted for testing of all beams with a/d ratio of 4.5. All beams have thickness and span of 10 inches and 11 ft respectively. Beams are designed in such a way that tensile flexure failure would occur before shear failure.

After testing it was observed that ACI design procedures may be applied to wide beams for flexure design but at high reinforcement ratios such beams may fail in shear at a load less than that predicted by ACI shear equations. Sudden shear mode of failure was observed for the beams which were reinforced closer to balanced reinforcement ratios. It was also noted that changing width did not change the mode of failure of wide beams.

TABLE OF CONTENTS

CONTENTS		PAGE NO
1	INTRODUCTION	
1.1	General	1
1.2	RC Wide Beams	1
1.3	Scope of Study	2
1.4	Objectives	2
1.5	Methodology	3
2	LITERATURE REVIEW	
2.1	General	4
2.2	Literature	4
3	EXPERIMENTAL PROGRAM AND DESIGN CALCULATIONS	
3.1	General	12
3.2	Mix Design	12
3.3	Materials	13
	3.3.1 Cement	13
	3.3.2 Fine Aggregate	13
	3.3.3 Course Aggregate	14
	3.3.4 Water	14
	3.3.5 Super plasticizer	14
3.4	Casting of beams	15
	3.4.1 Description of Specimens	16
3.5	Curing of Beams	17
3.6	Design calculations	18
	3.6.1 Material Strengths	18
	3.6.2 Reinforcing Steel	18
	3.6.3 Balanced Reinforcement Ratio	19
	3.6.4 Selection of Shear Span to Depth Ratio	20
	3.6.5 Theoretical Moment and Shear Capacities	22

	3.6.6 Effective Moment of Inertia and Theoretical Deflections	27
4	EXPERIMENTAL RESULTS	
4.1	Concrete Strength	34
4.2	Testing Setup	34
4.3	MEASUREMENTS	35
	4.3.1 Deflections	35
	4.3.3 Strains	35
4.4	Test Behavior of Specimens	36
	4.4.1 Specimen W1	36
	4.4.2 Specimen W2	39
	4.4.3 Specimen W3	41
	4.4.4 Specimen W4	43
	4.4.5 Specimen M1	45
	4.4.6 Specimen M2	47
	4.4.7 Specimen M3	49
	4.4.8 Specimen M4	51
4.5	Summary of Test Results	53
	4.5.1 W1, W2, M1 and M2	53
	4.5.2 W3, W4, M3 and M4	54
5	CONCLUSIONS AND RECOMMENDATIONS	
5.1	Behavior of Medium Reinforced Concrete wide Beams	56
5.2	Behavior of Highly Reinforced Concrete Wide Beams	56
5.3	Discussion	57
5.4	Conclusions	58
5.5	Recommendations	58
	APPENDIX I	61
	REFERENCES	93

LIST OF FIGURES

FIG No	TITLE
1.1	Description of all beams
2.1	Shear transfer mechanism for reinforced concrete members without web reinforcement
2.2	Derivation of ACI expression for diagonal cracking shear V_c
3.1	Casting of beams at NICE, NUST, Islamabad
3.2	Details of cross-section and reinforcement in beams
3.3	Curing of beams
3.4	Strain profile at balanced failure
3.5	Selection of shear span
3.6	Cross-sections of W1 and W2
3.7	Cross-sections of W3 and W4
3.8	Cross-sections of M1 and M2
3.9	Cross-sections of M3 and M4
4.1	Testing set-up
4.2	Testing set-up showing LVDT's
4.3	Demic points attached across the depth
4.4	Cracking pattern of W1
4.5	Deflected shape of W1
4.6	Load versus deflection graph of W1
4.7	Theoretical versus actual deflections of W1
4.8	Cracking pattern of W2
4.9	Deflected shape of W2
4.10	Load versus deflection graph of W2
4.11	Theoretical versus actual deflections of W2
4.12	Cracking pattern of W3
4.13	Picture showing the distance of shear crack from centre of support
4.14	Load versus deflection graph of W3
4.15	Deflected shape of W3
4.16	Theoretical versus actual deflections of W3

FIG No	TITLE
4.17	Cracking pattern of W4
4.18	Load versus deflection graph of W4
4.19	Deflected shape of W4
4.20	Theoretical versus actual deflections of W4
4.21	Cracking pattern of M1
4.22	Load versus deflection graph of M1
4.23	Deflected shape of M1
4.24	Theoretical versus actual deflections of M1
4.25	Cracking pattern of M2
4.26	Load versus deflection graph of M2
4.27	Deflected shape of M2
4.28	Theoretical versus actual deflections of M2
4.29	Cracking pattern of M3
4.30	Load versus deflection graph of M3
4.31	Deflected shape of M3
4.32	Theoretical versus actual deflections of M3
4.33	Cracking pattern of M4
4.34	Load versus deflection graph of M4
4.35	Deflected shape of M4
4.36	Theoretical versus actual deflections of M4
4.37	Combined behavior of all beams

LIST OF TABLES

TABLE	TITLE
3.1	Mix Design
3.2	Cement Properties
3.3	Properties of fine aggregates
3.4	Gradation of fine aggregates
3.5	Properties of coarse aggregates
3.6	Gradation of coarse aggregates
3.7	Technical data-Super plasticizer
3.8	Details of cross-sections and reinforcements
3.9	Compressive strength of cubes at 7, 14 and 28 days
3.10	Steel strengths of different bars used
3.11	Theoretical deflections of W1 and W2
3.12	Theoretical deflections of W3 and W4
3.13	Theoretical deflections of M1 and M2
3.14	Theoretical deflections of M3 and M4
4.1	Summary of test results of all beams

LIST OF NOTATIONS

d	effective depth of tensile reinforcement, in
c_b	depth of neutral axis, in (balanced)
ρ_b	balanced reinforcement ratio
a_b	depth of compression block, in (balanced)
f'_c	concrete compressive strength, psi
A_s	area of bottom tensile reinforcement, in ²
A'_s	area of top compression reinforcement, in ²
f_y	steel reinforcement grade, psi
b	width of beam, in
a'	shear span, in
P	design flexure load, kips
V_c	shear strength of concrete, kips
V_s	shear strength provided by stirrups, kips
ρ	tensile reinforcement ratio
ρ'	compression reinforcement ratio
c	depth of neutral axis, in
d'	depth of compression reinforcement, in
f'_s	stress in compression steel, ksi
A_v	area of shear reinforcement, in ²
s	spacing of shear reinforcement, in
A_c	concrete cross-section area, in ²
A_T	A _c + A _s + A' _s , in ²
y	geometric centroid of beam cross-section, in
I_g	gross moment of inertia of beam, in ⁴
M_{cr}	cracking moment, kip-ft
y'	centroid of cracked beam section, in
n	modular ratio
I_g	cracked moment of inertia, in ⁴
I_{eff}	effective moment of inertia, in ⁴

Chapter-1

INTRODUCTION

1.1 General

A beam is a structural member that transfers load from slab to the columns and ultimately, from columns load is transferred to foundation or ground. A beam is designed to take loads acting perpendicular to its longitudinal axis. Under a load beam encounters two internal forces i.e. moment or stress resultant and shear force. Load transfer mechanism in a beam depends on many factors like span to depth ratio, shear span, beam geometry, support conditions and loading conditions etc. Concrete materials have given us the advantage to cast any form and shape of desired structural members. With the introduction of steel in concrete as a reinforcing material its performance in taking tensile forces can be enhanced to a greater extent. Concrete possesses significant resistance against compressive forces but it is weaker in resisting tensile forces. Steel is efficient in resisting both tensile and compressive stresses. Therefore, reinforced concrete members can be used to efficiently utilize both tensile and compressive strengths of the two materials in a single matrix.

1.2 Reinforced Concrete Wide Beams

Wide beam is generally defined as a beam whose width is at least twice its depth. Such beams are recognized in building construction by the fact that their depth is almost equal to that of the floor above them. In the modern construction practice architectural requirements have given rise to the frequent use of wide beams as a load transfer element. Because of their smaller depth wide beams reduce the floor height resulting in larger number of stories in a given height and aiding the installation of different services under the floor. Another important factor which encourages the use of wide beams is that they curtail the construction cost because of the easiness associated with the form works. In this regard there is a concern that flexure and shear provisions for wide beams can be unsafe hence it is not widely agreed that design procedures of narrow beams are equally applicable to wide beams.

1.3 Scope of Study

Scope of this research is to study flexural and shear behavior of reinforced concrete wide beams. ACI code provides design procedures for normal dimensioned beams but there is no specific design methodology for RC Wide beams available in ACI code. Study encloses the testing of eight full scale reinforced concrete wide beams with different width and same reinforcement ratio and vice versa. All beams were designed under balance reinforcement conditions and had a constant thickness of 10 inches. Shear failure was secured to let the beam fail in flexure. Maximum spacing of shear reinforcement was limited to $d/2$. Shear reinforcement configuration in all beams was 4 legged #2 & #3 bars. Beams were tested under four point bending method and shear span was selected in such a way that the beam to be tested best resembles to a uniformly loaded beam.

1.4 Objectives

- To study new insights of overall structural behavior of RC wide Beams
- To study applicability of normal design procedures for reinforced concrete wide beams
- To study the flexure-shear behavior at high reinforcement ratios
- To study load deflection response of medium and highly reinforced concrete wide beams
- To study the ultimate shear strength and modes of failure of wide beams with medium and high longitudinal reinforcement ratios with web reinforcement.

1.5 Methodology

Casting and testing was performed at NICE, NUST. Eight beams were divided into two series i.e. W and M series. W series contained 30 inches wide beams while M series consisted of 40 inches wide beams. Depth of all beams was kept 10 inches. In each series longitudinal reinforcement ratio was the variable while between two series width of beam was the variable. Four point bending method was used for testing of beams. Shear span to depth ratio of 4.5 was maintained for all beams. Figure 1.1 shows the nomenclature of all beams

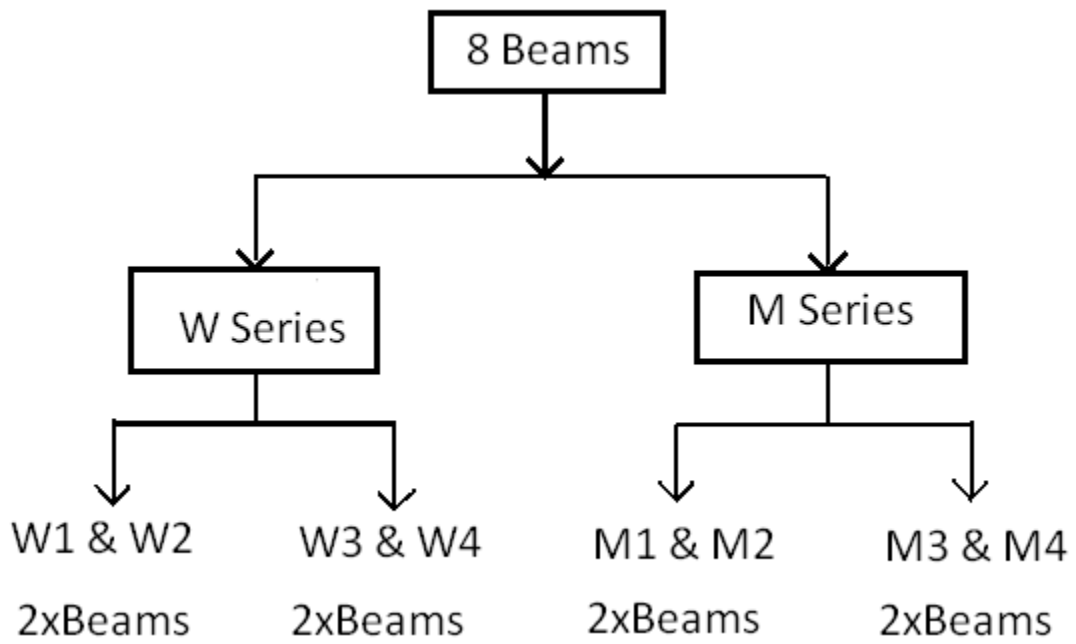


Fig 1.1 Descriptions of All Beams

Chapter-2

LITERATURE REVIEW

2.1 General

A beam transfers its load to supports by flexure and shear mechanisms. Flexure design is based on the Bernoulli beam theory which is based on the assumption that plane section remains plane before and after bending, assuming a linear profile of longitudinal strains across the depth of beam. Design moment capacity is calculated using Whitney stress block method. Shear strength of concrete beam is calculated using empirical equation given in ACI-318-14 section 22.5.5.1. Many studies have been conducted to find out the ultimate shear capacity of RC wide beams but there is almost no research found regarding flexure behavior of RC wide beams. There is a general agreement among researchers on the mechanisms that participate in carrying shear loads over the cross section as shown in Fig. 2.1. In the light of the findings of the state-of-the-art reports by the joint ASCE-ACI Committee 426 [3] and 445 [4], the shear transfer mechanisms involve the following parts: (1) the shear stresses in uncracked concrete, e.g., the flexural compression zone; (2) the interface shear transfer, often called aggregate interlock or crack friction; (3) the dowel action of the longitudinal reinforcing bars; (4) the arch action; and (5) the residual tensile stresses transmitted directly across cracks.

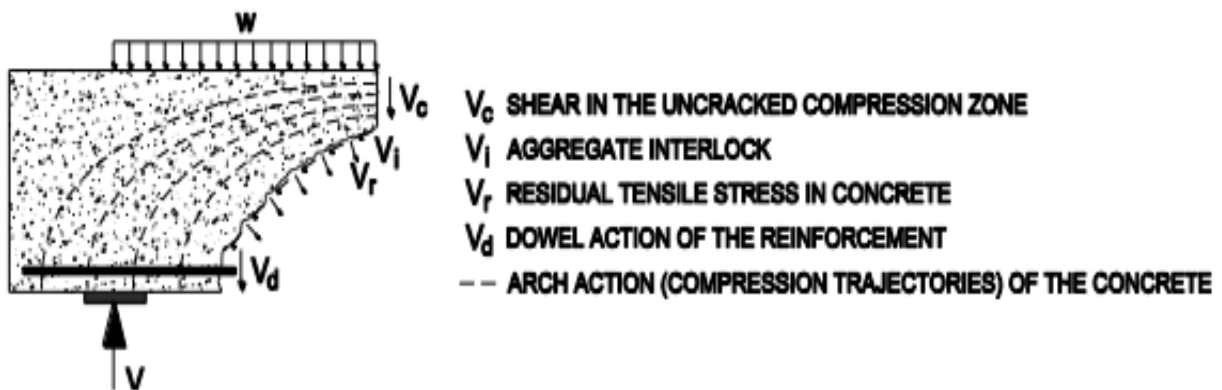


Fig. 2.1-Shear transfer mechanism for RC members without web reinforcement

(Adapted from reference 10)

2.2 Literature Review

There is now substantial evidence²⁻⁶ that for members without stirrups, the shear stress at failure decreases as the member becomes larger and as the percentage of longitudinal reinforcement becomes lower. Unfortunately when the basic ACI shear design provisions⁷ were being formulated about 50 years ago, the sensitivity of failure shear stress to size and reinforcement ratio was not recognized. The basic expression for shear strength V_c derived at the time was intended to present the lower portion of experimental scatter band. fig. 2.2 which is from the 1926 ACI-ASCE Committee 326 report⁸, shows only four of the 194 test results falling below the usual estimate of V_c which is $2\sqrt{f_c} bd$.

The average depth of the beam shown in fig. 2.1 was 13.4 in and the average longitudinal reinforcement ratio was 2.22 percent. When these expressions are applied to larger members that contain lower percentages of reinforcement, the estimates of failure may be much less conservative.

Thomas et al. carried out an experimental study⁹ on cyclic behavior of both narrow and wide beams. A 20 story, four bay interior transverse frame of a reinforced concrete office building was designed as a prototype frame. Behavior of longitudinal unconfined bars outside the column was studied and it was concluded that in beam column joint with narrow and wide beams, the longitudinal bars outside the joint offered a significant contribution to the lateral resistance and energy dissipation.

An experimental investigation¹⁰ was conducted by Collins et al. to evaluate the significant parameters that influence the magnitude of size effect in shear. Decrease in shear stress at failure as the member size becomes large, is called size effect. Study involved the testing of 22 simple span beams, 12 continuous beams and one large frame. Point load was applied at mid span of beam resulting in a shear span to depth ratio of 3. Thirteen of the beams had an overall depth of 39.4 in, four had an overall depth of 19.7 in, and four had an overall depth of 9.8 in while one had an overall depth of 4.9 in. longitudinal reinforcement ratio varied from 1.19 percent down to 0.5 percent. It was observed that reduction in shear stress at failure was related more directly to the maximum spacing between the layers of longitudinal reinforcement rather than the overall

member depth and ACI shear provisions can be unsafe when applied to large lightly reinforced members.

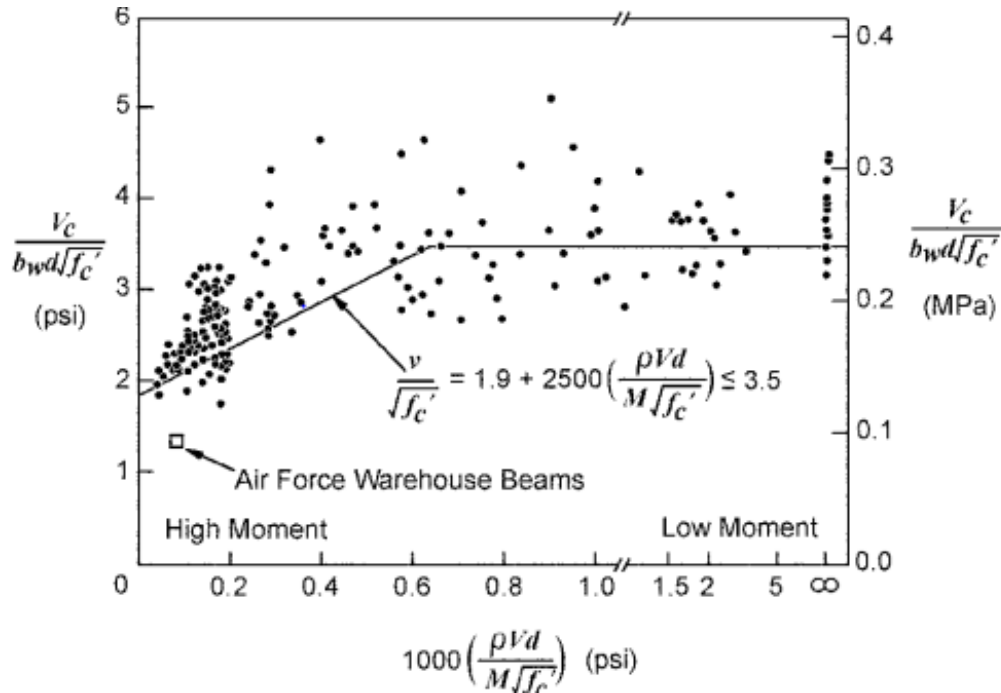


Fig. 2.2– Derivation of ACI expression for diagonal cracking shear V_c (adapted from Reference 7)

Frosch et al. tested six beams with primary variables being beam size and stirrup spacing at Purdue University¹¹. For the beams tested in their study, beam size and stirrup spacing did not influence the angle at which primary cracking occurred. Moreover, as the longitudinal reinforcement ratio was decreased, there was an observed reduction in concrete shear strength. Lubell et al.¹² studied the size effect in wide beams and suggested that minimum shear reinforcement could not be ignored for wide beams. They proposed changes in ACI shear provisions for wide beams. It was demonstrated that by applying the provisions for wide beam, a prototype large wide specimen fully conforming to the ACI 318-05 provisions could fail at a load less than the corresponding design service load in shear. Collins et al.¹³ conducted an experimental study on one way shear strength of thick slabs and wide beams. Based on experimental results the study concluded that the ACI shear provisions can result in inadequate levels of safety for both thick slabs and wide beams. In another study Lubell et al.¹⁴

demonstrated that in members with no shear reinforcement, both the member depth and the details of longitudinal flexural reinforcement influence the shear capacity of the member.

In recent research¹⁵⁻¹⁶ there have been studies to evaluate and propose a practical and optimum arrangement of shear reinforcement for wide members and to compare against the codes.

Most of the building codes in the middle east; the current Egyptian Code of practice (ECP 203-2007) for example, require that the applied one way shear stress in the shallow wide beams be less than the concrete shear strength without any shear reinforcement contribution, and the shear strength provided by concrete equals two thirds of concrete shear strength of shallow slender beams. As a consequence; a large cross-sectional areas of concrete shall be provided for these members to resist one-way shear demands which results in a conservative uneconomic design provision. The above mentioned requirements by some building codes in the Middle East were not found in most of other recognized international codes or standards. An experimental program¹⁷ was carried out to investigate the contribution of web shear reinforcement to shear strength of shallow wide beams. The main parameters considered in this investigation were: concrete compressive strengths and vertical stirrups; with varying amount, configuration and spacing. The experimental program consisted of twelve simply-supported reinforced concrete wide beams subjected to two concentrated loads at third points. The specimens were divided into 5 groups. All specimens were typically proportioned so that shear failure would preclude flexural failure. Shear strengths at failure recorded in this experimental program were compared to the analytical strengths calculated according to some international codes. Test results clearly demonstrated the significance of the web reinforcement in improving the shear capacity the ductility of the shallow wide beams which was consistent with the recognized international codes and standard provisions. Lofty et al.¹⁸ carried out an experimental program to investigate the contribution of shear reinforcement to shear strength, shear cracks, ductility and mode of failure of shallow wide concrete beams. The main parameters considered in this research were: shear reinforcement ratio, shear span to depth ratio (a/d), spacing between stirrups and number of vertical branches, spacing between stirrups to depth ratio (s/d). Experimental program consisted of ten simply supported reinforced concrete wide beams. Specimens were divided into two groups each consists of 5 beams, one control beam without shear reinforcement and four beams with shear reinforcement. The shallow wide beams were subjected to two concentrated loads

with $(a/d) = 3&4$ for the first group and the $(a/d) = 2&5$ for the second group. It was observed that both ductility and shear strength increased by increasing web reinforcement ratio. It is important that shear strength varied inversely with the shear span to depth ratio. Code provisions for one-way shear assume a linear relation between the shear capacity of a reinforced concrete member and its width. For wide members subjected to a concentrated load, an effective width in shear should be introduced. To study the effective width and the influence of the member width on shear capacity, a series of experiments¹⁹ was carried out on continuous one-way elements of different widths. The size of the loading plate, the moment distribution at the support, and the shear span-depth ratio were varied and studied as a function of the member width. It was found that, as width of the beam increased, the effect of size of loading plate increased while the influence of shear span to depth ratio decreased. This finding can be explained by understanding that a three dimensional load carrying mechanism is developed in wider beams in contrary to that of two dimensional load carrying mechanism in narrow beams. Yasouj et al.²⁰ tested six wide beams to investigate the effectiveness of different types of shear reinforcement in improving the shear capacity of wide beams. One specimen each was provided: without vertical stirrups, with vertical stirrups, independent bent-up bars, independent mid-depth horizontal bars and the combination of vertical stirrups and bent up bars. It was observed that using independent bent-up bars significantly improved the shear capacity of wide beams. Independent horizontal bars increased the shear capacity to some extent, but the beam was less ductile through the failure. The combination of independent bent-up bars with stirrups led to higher shear capacity and gradual failure of the specimens. The result also indicated that the beam with banded main reinforcement achieved a larger failure load than did the beam with evenly distributed bars.

Shear behavior of reinforced concrete wide beams was studied by Elrakib and Said²¹. The experiment consisted of nine beams of 29 MPa concrete strength tested with a shear span to depth ratio equal to 3.0. One of the tested beam had no web reinforcement as a control specimen. The flexure mode of failure was secured for all the specimens to study the shear mode of failure. The key parameters involved were effect of existence, spacing, amount and yield strength of vertical stirrups on shear capacity and ductility of the tested wide beams. Study showed that the contribution of web reinforcement to the shear capacity was significant and directly proportional to the amount and spacing of shear reinforcement. The increase in the shear capacity ranged from 32% to 132% for the range of tested beams compared with control beam. High grade steel was

more effective in contribution of shear strength of wide beams. Also, test demonstrated that the shear reinforcement significantly enhanced the ductility of wide beams.

In order to study both the shear and flexural behavior of wide beams and evaluate the possibility of substituting the minimum conventional transverse reinforcement required by Euro code 2 with steel fibers, full-scale beams were tested²². Specimens, all 250 mm deep, had two different widths, fiber contents and also, minimum amount of classical shear reinforcement. Results evidenced that a relatively low volume fraction of fibers can significantly increased shear bearing capacity and beam ductility. Moreover, wide beams did not show the typical brittle failure in shear, even without any shear reinforcement, as the effect of fibers was more prominent than in deep beams. Peculiarities of wide beams were evidenced in terms of enhancements both in shear and in flexure. Experimental results were evaluated in terms of strength, ductility, post-cracking stiffness, shear and flexural cracking, collapse mechanism and fiber effect. The ultimate bearing capacity observed in shear was 20-25% greater than expected and the failure was associated with a visible warning, cracking and deflections. Width to effective depth ratio of wide beams seemed to significantly influence the mechanism of failure and the bearing capacity, with positive implications both in shear and flexure. Either minimum shear reinforcement or fibers, in relatively low amount, greatly influenced the shear behavior of wide beams, basically by delaying the occurrence of the shear failure mechanism and, eventually, by altering the collapse from shear to flexure, with enhanced bearing capacity and ductility. Steel fibers, even in small amount, improved the behavior of wide beams at service load state, by reducing deflection (increasing the tension-stiffening effect) and crack width.

Shuraim and Ahmed²³ addressed the influence of stirrup configurations in wide beams on the effectiveness of stirrups in contributing to shear resistance as a ratio of the nominal shear stirrup strength. The evaluation was made by testing 16 continuous, wide, shallow, reinforced, concrete beams supported on interior narrow columns at their centers and simply supported at the ends. The 16 beams were composed of: three beams without stirrups, six beams having a constant amount of stirrups with either two-leg or four-leg configuration, and seven other beams with various configurations to verify the trend. The general trend was that reducing the transverse spacing of stirrups improves the stirrup efficiency to resist shear forces. For beams with a constant amount of stirrups, four-leg configuration showed a high increase in its

efficiency to resist shear force over stirrups with two-leg configuration. Although code design equations assume that stirrups are fully effective, it was evident that wide shallow beams reinforced with two-leg stirrups were susceptible to becoming shear deficient if transverse spacing was not accounted for.

In view of all above studies discussed, it can be seen that there is a diversity in assessing the shear strength of reinforced concrete wide beams indicating the need of further research to be done to understand the shear mechanism. Current research is an attempt to study combined flexure-shear behavior of shear secured concrete wide beams at different reinforcement ratios. Because of less relative stiffness, wide beams undergo larger deflections when provided in structural floor systems. Deflections can be controlled by providing max possible longitudinal reinforcement ($\rho \leq \rho_b$) in thin wide beams. There are two series of beams: W series is 30 in wide and M series is 40 in wide. In each series, there are three longitudinal reinforcement ratios i.e. $0.59\rho_b$, $0.65\rho_b$ and $0.95\rho_b$. All beams have been provided with shear reinforcement to secure the shear failure so as to test a flexure controlled wide beam.

Chapter -3

EXPERIMENTAL PROGRAM AND DESIGN CALCULATIONS

3.1 General

Experimental program consists of testing of eight Reinforced Concrete Wide Beams. Eight beams comprise of two different series of RC Wide beams being W and M. W series refer to 30 inches wide beams and M series belongs to 40 inches wide beams. Reinforcement ratio is the variable in each series while beam width is the variable among the two series. Hence, there are two different possibilities

1. Beams with same width and different reinforcement ratio
2. Beams with almost equal reinforcement ratio and different width

All beams are designed as under reinforced beams with three different ρ/ρ_b ratios being 0.59, 0.63 and 0.95. Wide beams are more prone to large deflections therefore, 2 beams from each series are designed as doubly reinforced sections intentionally to observe their overall behavior. Shear reinforcement was provided as per ACI provisions in such a way that flexure failure occurs before shear failure with a minimum margin of 28%.

3.2 Mix Design

In the study, f'_c selected was 4000 psi. Mix design is tabulated below.

Description	Details
Cement	450 kg / m ³
Fine Aggregate	760 kg / m ³
Course Aggregate	1040 kg / m ³
W/C Ratio	0.41
Supper Plasticizer (Ultra Superplast 470)	0.9% by weight of cement
Mix Ratio	1 : 1.69 : 2.31

Table 3.1 Mix Design

3.3 Materials

3.3.1 Cement

The type I cement conforming to ASTM C 150 – 04 was used. Results of cement properties are formulated below in Table 3.2.

Tests	Test Results	Specifications
Specific Gravity	3.15	ASTM C 188-95
Initial Setting Time	170 minutes at 17° C	ASTM C 191-01
Final Setting Time	330 minutes at 17° C	ASTM C 191-01

Table 3.2 Cement Properties

3.3.2 Fine Aggregate

Locally available sand was used. Results of tests performed to find out the properties of sand are formulated in Table 3.3. The size distribution of fine aggregate is shown in Table 3.4. Fineness modulus of sand was determined to be 2.51.

Tests	Test Results	Specifications
Specific Gravity	2.6	ASTM C 128 – 01
Absorption	1.1 %	ASTM C 128 – 01
Fineness Modulus	2.51	ASTM C 33 - 02

Table 3.3 Properties of Fine Aggregate

Sieve No	Weight Retained (gm)	Percent Retained	Cumulative Percent Retained	Percent Passing	
				Actual	ASTM C 33 - 02
#4	2	0.2	0.2	99.8	95-100
#8	16	1.6	1.8	98.2	80-100
#16	134	13.4	15.2	84.8	50-85

#30	320	32	47.2	52.8	25-60
#50	425	42.5	89.7	10.3	5-30
#100	70	7	96.7	3.3	0-10
Sieve No	Weight Retained (gm)	Percent Retained	Cumulative Percent Retained	Percent Passing	
				Actual	ASTM C 33 - 02
#200	31	3.1	99.8	0.2	
pan	2	0.2	100	0	

Table 3.4 Gradation of Fine Aggregate

3.3.3 Course Aggregate

Course aggregate was taken from Margalla crush site with a maximum size of 12.7 mm. Tests results on the course aggregate are shown in table 3.5. The gradation and sieve analysis were performed in unison with ASTM C 136 – 01 and formulated in Table 3.6.

Detail of Test	Test Results
Impact value (percent)	11.3
Crushing value (percent)	21.2
Abrasion Value (percent)	15.7
Specific Gravity	2.6

Table 3.5 Properties of Course Aggregate

Sieve Size (mm)	Weight Retained (gm)	Percent Retained	Cumulative Percent Retained	Percent Passing	
				Actual	ASTM C 33 - 02
19	0	0	0	100	100
12.5	78	7.8	7.8	92.2	90-100
9.5	410	41	48.8	51.2	40-70
4.75	488	48.8	97.6	2.4	0-15
2.36	24	2.4	100	0	0-5

Table 3.6 Gradation of Course Aggregate

3.3.4 Water

For mixing and curing of Concrete, drinkable water was used.

3.3.5 Super plasticizer

Superplast 470, a high performance concrete super plasticizer was used in the mix. A constant quantity of 0.9% by weight of cement was maintained in the study. The technical details of superpalst 470 are tabulated below

Description	Details
Name	Ultra Superplast 470
Form	Viscous Liquid
Color	Brown
Specific Gravity	1.19 at 20° C
Alkali Content (%)	Less than 72g
Chloride Content (%)	Nil to BS 5075
Air Entrained	Less than 2 %

Table 3.7 Technical Data – Super plasticizer

3.4 Casting of Beams

Eight Beams were cast with single batch of concrete having capacity of 7 cum procured from a batching plant. Pouring and casting was performed at NICE, NUST on December 19, 2014. Twelve 6” x 6” concrete cubes were also cast at the time of pouring for determination of compressive strength.



Fig 3.1-Casting of Beams at NICE, NUST, Islamabad.

3.4.1 Description of Specimens

Study encloses the Flexural and Shear behavior of eight reinforced concrete wide beams ($b/h \geq 2$). Eight beams are divided into two series i.e. W and M. Four beams in W series are 30" wide while other four are 40" wide. All beams have a constant thickness of 10". Beams are designed in such a way that flexure (tensile) failure occurs before shear failure. Shear reinforcement was provided throughout the span and maximum spacing was limited to $d/2$. The details of each specimen is shown in the table below

Beam Description	Effective Depth (in)	Tensile Reinforcement	Shear Reinforcement	ρ	ρ/ρ_b	Theoretical Failure load P (Kips)	Theoretical Shear Strength (Kips)
30" x 10" (W1)	7.75	4#8 bars	#2@3.75" c/c Four legged	0.0136	0.63	43.45	46.5
30" x 10" (W2)	7.75	4#8 bars	#2@3.75" c/c Four legged	0.0136	0.63	43.45	46.5
30" x 10" (W3)	7.625	8#8 bars	#3@3.5" c/c Four legged	0.0276	0.95	67.33	89.80
30" x 10" (W4)	7.625	8#8 bars	#3@3.5" c/c Four legged	0.0276	0.95	67.33	89.80
40" x 10" (M1)	7.75	5#8 bars	#2@3.75" c/c Four legged	0.0127	0.59	54.79	56.5
40" x 10" (M2)	7.75	5#8 bars	#2@3.75" c/c Four legged	0.0127	0.59	54.79	56.5
40" x 10" (M3)	7.625	10#8 bars	#3@3.75" c/c Four legged	0.0259	0.95	85.33	95.7
40" x 10" (M4)	7.625	10#8 bars	#3@3.75" c/c Four legged	0.0259	0.95	85.33	95.7

Table 3.8 Detail of Cross-sections and Reinforcement

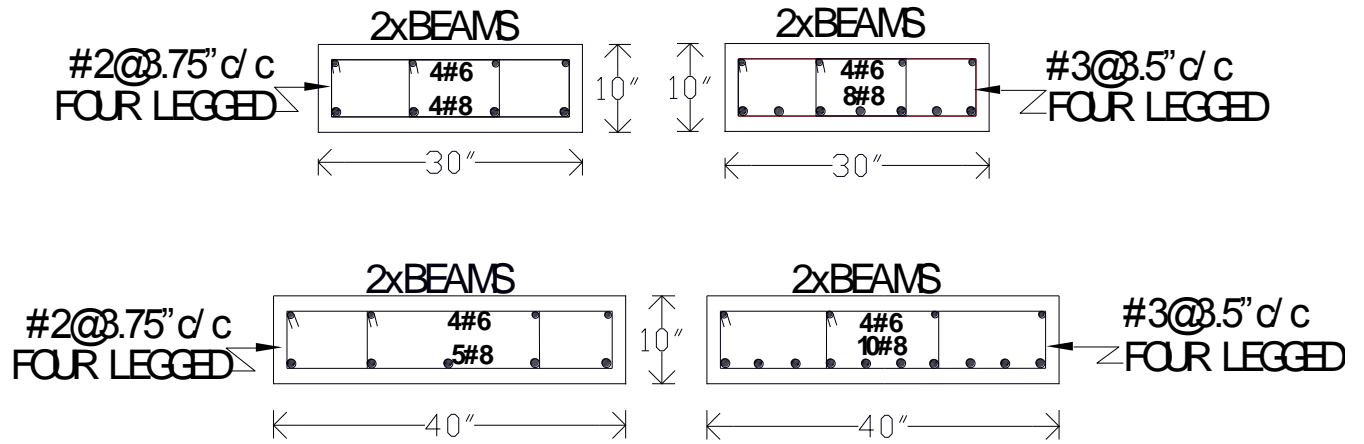


Fig 3.2 Details of Cross Section and Reinforcement

3.5 Curing of Beams

Hessian cloth was placed on surface of beams and it was kept wet during daytime. Cubes were also cured in the same condition as that of Beams. Potable water was used for curing purpose.



Fig3.3 Curing of Beams

3.6 Design Calculations

3.6.1 Material Strengths

Twelve concrete cubes of 6" x 6" were cast at the time of pouring. Compressive strengths of cubes determined from testing at different age of curing are given in table 3.9. Compressive strength of cylinder is taken as 0.87 times that of a cube.

Size of Cube	Testing Day	f _c (psi)
6" x 6"	7	3305
6" x 6"	7	3278
6" x 6"	14	4041
6" x 6"	14	4087
6" x 6"	28	4772
6" x 6"	28	4790

Table 3.9 Compressive Strength of Cubes at 7, 14 and 28 Days

Compressive strength of cylinder determined on testing day
= $0.87 \times 4790 = 4160 \text{psi}$

3.6.2 Reinforcing Steel

Longitudinal Steel consisted of #8 and #6 bars. #8 bars were used as main tensile reinforcement in all beams while #6 bars acted as hangers in singly reinforced beams i.e. W1, W2, M1 and M2. #2 and #3 bars were used as transverse shear reinforcement. Grade 60 steel was used for all types of longitudinal reinforcement. The only grade 40 steel was #2 bars used as shear reinforcement of lightly reinforced beams i.e. W1, W2, M1 and M2. Steel was tested using specifications in line with ASTM 615. Actual Yield strengths determined from tests for different diameters are written as under

Bar No.	Nominal Diameter (in)	Measured Diameter (in)	Weight (Lb/ft)	Area (in ²)	Yield Strength (ksi)	Ultimate Strength (ksi)
#3	3/8	0.374	0.374	0.11	64	82.67
#3	3/8	0.375	0.378	0.11	62	80.63
#6	6/8	0.75	1.502	0.441	60.50	101.21
#6	6/8	0.75	1.502	0.441	63.50	102.33
#8	1	1.008	2.679	0.78	74.5	99.71
#8	1	1.008	2.678	0.78	75.5	100

Table 3.10 Steel Strength of Different Bars used

Yield strengths used in calculations are 40ksi, 63ksi, 62ksi and 75ksi for #2, #3, #6 and #8 bars respectively.

3.6.3 Balanced Reinforcement Ratio

ρ_b for “Effective Depth = 7.75”

Effective Depth $d = 10 - 1.5 - 0.5 - 0.25 = 7.75$ in

Considering balance failure, at ultimate, the strain profile will be as under

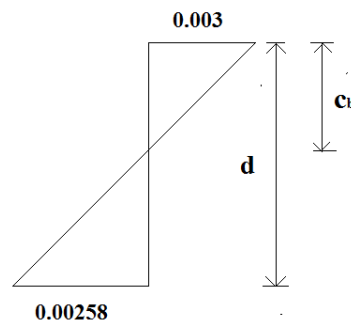


Fig3.4 Strain Profile at Balanced Failure

From similar triangles

$$\frac{Cb}{0.003} = \frac{d - Cb}{0.00258}$$

$$C_b = 4.16 \text{ in}$$

Depth of compression block “ a_b ” = $0.85 * 4.16 = 3.54 \text{ in}$

$$\rho_b = (0.85 * f_c' * a_b) / (f_y * d)$$

$$\rho_b = 0.0215$$

ρ_b for “Effective Depth = 7.625”

Effective Depth $d = 10 - 1.5 - 0.5 - 0.375 = 7.625 \text{ in}$

$$C_b = 4.1 \text{ in}$$

Depth of compression block “ a_b ” = $0.85 * 4.1 = 3.48 \text{ in}$

$$\rho_b = (0.85 * f_c' * a_b) / (f_y * d)$$

$$\rho_b = 0.0215$$

3.6.4 Selection of shear span to depth ratio (a'/d)

Load transfer mechanism in a beam is largely dependent on a'/d ratio. Generally, to study shear behavior a'/d of 2.5 or below is selected. Any a'/d ratio above 2.5 will be representing flexure governing mechanism. In this study the value of shear span is selected in such a way that the beam to be tested best resembles with an actual beam which is uniformly loaded. Working for selection of shear span is shown below

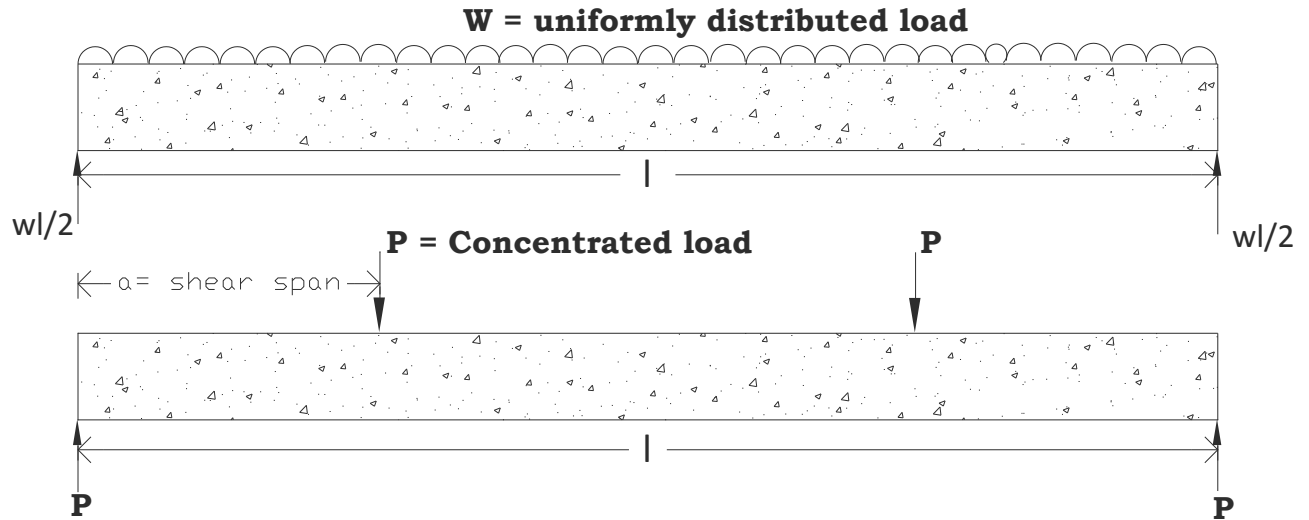


Fig3.5 Selection of Shear Span

Equating the maximum applied moment and applied shear we get

$$P = \frac{wl}{2}$$

$$Pa = \frac{(wl) * l}{8} = \frac{2P * l}{8} = \frac{Pl}{4}$$

$$\text{It gives } a = \frac{l}{4}$$

Since all beams had an effective span of 11 ft. therefore,

$$\text{Shear span} = \frac{11 * 12}{4} = \mathbf{33 \text{ inches}}$$

Actual value of shear span provided was taken as 34.875 inches to ensure the happening of flexure failure before shear failure.

3.6.5 Theoretical Moment and Shear Capacities

W1 & W2

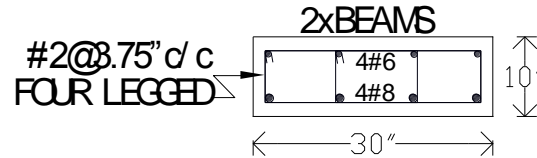


Fig3.6 Cross-section of W1 & W2

$$\text{Tension Reinforcement Ratio} = \frac{4 \cdot 0.79}{30 \cdot 7.75} = 0.0136 < \rho_b \text{ (under reinforced)}$$

$$A_s = 3.16 \text{ in}^2$$

$$\begin{aligned} \text{Depth of compression block } a &= (A_s \cdot f_y) / (0.85 \cdot f'_c \cdot b) \\ &= (3.16 \cdot 75) / (0.85 \cdot 4.16 \cdot 30) = 2.23 \text{ inches} \end{aligned}$$

$$\begin{aligned} \text{Moment Capacity of W1 \& W2} &= A_s \cdot f_y \cdot (d - a/2) \\ &= (3.16 \cdot 75) \cdot (7.75 - 2.23/2) = 1572.5 \text{ k}'' \end{aligned}$$

Moment Capacity of W1 & W2 = 131 k-ft

$$\text{Self weight of beam} = 30 \cdot 10 \cdot 0.15 / 144 = 0.313 \text{ k/ft}$$

$$\text{Moment due to self weight} = 4.73 \text{ k-ft}$$

Now equating the applied moment with moment capacity we obtain

$$(34.875/12) \cdot P + 4.73 = 131$$

$$\text{Gives } P = 43.45 \text{ kips} = \mathbf{19.71 \text{ tons}}$$

$$\begin{aligned} \text{Shear Strength} &= V_c + V_s = 2 \cdot \sqrt{f'_c} \cdot b \cdot d + \frac{A_v \cdot f_y \cdot d}{s} \\ &= 2 \cdot \sqrt{4160} \cdot 30 \cdot 7.75 + \frac{4 \cdot 0.05 \cdot 40 \cdot 7.75}{3.75} = 46.5 \text{ kips} \end{aligned}$$

Shear Strength of W1 & W2 = **21 tons** (shear failure secured)

W3 & W4

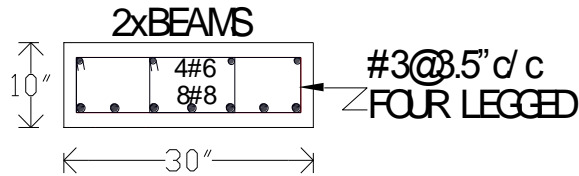


Fig3.7 Cross-section of W3 & W4

$$\text{Tension Reinforcement Ratio} = \frac{8 \cdot 0.79}{30 \cdot 7.625} = 0.0276 > \rho_b \text{ (Doubly reinforced)}$$

$$A_s = 6.32 \text{ in}^2$$

$$A'_s = 4 \cdot 0.44 = 1.76 \text{ in}^2$$

$$\rho'_b \text{ (Balanced Reinforcement Ratio for Doubly Reinforced Section)} = \rho_b + \rho'$$

$$\rho'_b = 0.0215 + 0.00769 = 0.0292$$

$$\rho' = \frac{A'_s}{b \cdot d} = \frac{4 \cdot 0.44}{30 \cdot 7.625} = 0.00769$$

Since $\rho < \rho'_b$ So, tensile steel yields (under-reinforced)

From Equilibrium

$$T = C + C'$$

$$A_s \cdot f_y = 0.85 \cdot f'_c \cdot 0.85 \cdot c \cdot b + A'_s \cdot f'_s$$

$$\text{And } f'_s = 87 \cdot \left(\frac{c - d'}{c} \right)$$

$$d' = 2.25 \text{ in}$$

$$b = 30 \text{ in}$$

Upon solving we get "c" = 4.42 in

Which gives $f'_s = 42.71 \text{ ksi} < 62 \text{ ksi}$

So compression steel does not yield

$$\begin{aligned}
 \text{Moment Capacity of W3 \& W4} &= (A_s - A'_s) * f_y * (d - a/2) + A'_s * f'_s * (d - d') \\
 &= (6.32 - 1.76) * (75) * (7.625 - 3.76 / 2) \\
 &\quad + 1.76 * 42.71 * (7.625 - 2.25) \\
 &= 2370 \text{ k-inches} = 197.53 \text{ k-ft}
 \end{aligned}$$

Moment Capacity of W3 & W4 = 197.53 k-ft

Moment due to self weight = 5 k-ft

Now equating the applied moment with moment capacity we obtain

$$(34.313/12) * P + 4.73 = 197.53$$

Gives P = 67.33 kips = **30.55 Tons**

$$\begin{aligned}
 \text{Shear Strength} &= V_c + V_s = 2 * \sqrt{f'_c} * b * d + \frac{A_v * f_y * d}{s} \\
 &= 2 * \sqrt{4160} * 30 * 7.625 + \frac{4 * 0.11 * 63000 * 7.625}{3.5} = \mathbf{89.8 \text{ kips}}
 \end{aligned}$$

Shear Strength of W3 & W4 = **40.75 Tons** (shear failure secured)

M1 & M2

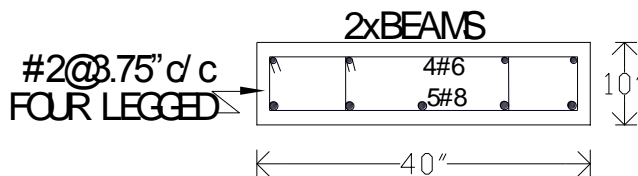


Fig3.8 Cross-section of W5 & W6

$$\text{Tension Reinforcement Ratio} = \frac{3.95}{40 * 7.75} = 0.0127 < \rho_b \text{ (under reinforced)}$$

$$A_s = 3.95 \text{ in}^2$$

$$\begin{aligned}
 \text{Depth of compression block } a' &= (A_s * f_y) / (0.85 * f'_c * b) \\
 &= (3.95 * 75) / (0.85 * 4.16 * 40) = 2.09 \text{ inches}
 \end{aligned}$$

$$\text{Moment Capacity of M1 \& M2} = A_s * f_y (d-a/2)$$

$$= (3.95*75) (7.75 - 2.09 /2) = 1986.35 \text{ k''}$$

Moment Capacity of M1 & M2= 165.53 k-ft

Moment due to self weight = 6.3 k-ft

Now equating the applied moment with moment capacity we obtain

$$(34.875/12)*P +6.3 = 165.53$$

Gives P = 54.79 kips = **24.86 Tons**

$$\text{Shear Strength} = V_c + V_s = 2 * \sqrt{f'c} * b * d + \frac{A_v * f_y * d}{s}$$

$$= 2 \sqrt{4160} * 40 * 7.75 + \frac{4*0.05*40000 *7.75}{3.75} = \mathbf{56.5 \text{ kips}}$$

Shear Strength of M1 & M2 = **25.6 Tons** (shear failure secured)

M3 & M4

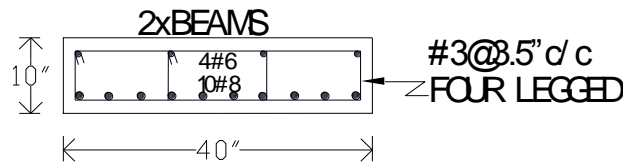


Fig3.9 Cross-section of W7 & W8

$$A_s = 7.9 \text{ in}^2$$

$$A'_s = 4*0.44 = 1.76 \text{ in}^2$$

$$\rho = \frac{7.9}{40*7.625} = 0.0259 > \rho_b \text{ (Analyze it as doubly reinforced section)}$$

$$\rho'_b \text{ (Balanced Reinforcement Ratio for Doubly Reinforced Section)} = \rho_b + \rho'$$

$$\rho'_b = 0.0215 + 0.00577 = 0.0273$$

$$\rho' = \frac{A'_s}{b*d} = \frac{4*0.44}{40*7.625} = 0.00577$$

Since $\rho < \rho'_b$ So, tensile steel yields (under-reinforced)

From Equilibrium

$$T = C + C'$$

$$A_s * f_y = 0.85 * f'_c * 0.85 * c * b + A'_s * f'_s$$

$$\text{And } f'_s = 87 * \left(\frac{c - d'}{c} \right)$$

$$d' = 2.25 \text{ in}$$

$$b = 40 \text{ in}$$

Upon solving we get “c” = 4.32 in

Which gives $f'_s = 41.68 \text{ ksi} < 62 \text{ ksi}$

So compression steel does not yield

$$\begin{aligned} \text{Moment Capacity of M3 \& M4} &= (A_s - A'_s) * f_y * (d - a/2) + A'_s * f'_s * (d - d') \\ &= (7.9 - 1.76) * (75) * (7.625 - 3.672 / 2) \\ &\quad + 1.76 * 41.68 * (7.625 - 2.25) \\ &= 3060 \text{ Kip-inches} = \mathbf{255 \text{ k-ft}} \end{aligned}$$

Moment due to self weight = 7 k-ft

Now equating the applied moment with moment capacity we obtain

$$(34.313/12) * P + 6.3 = 255$$

$$\text{Gives } P = 86.96 \text{ kips} = \mathbf{39.46 \text{ Tons}}$$

$$\begin{aligned} \text{Shear Strength} &= V_c + V_s = 2 * \sqrt{f'_c} * b * d + \frac{A_v * f_y * d}{s} \\ &= 2 * \sqrt{4160} * 40 * 7.625 + \frac{4 * 0.11 * 63000 * 7.625}{3.75} = 95.7 \text{ kips} \end{aligned}$$

Shear Strength of M3 & M4 = **43.42 Tons**

3.6.6 Calculations for Effective Moment of Inertia

Purpose of these calculations is to compute theoretical deflections and compare it with experimental deflections. Formula for calculating effective moment of inertia is taken from ACI-318. Detailed calculations are shown below.

W1 & W2

$$A_c = 300 \text{ in}^2$$

$$A_{st} = 3.16 \text{ in}^2$$

$$A'_{st} = 1.76 \text{ in}^2$$

$$A_T = 304.92 \text{ in}^2$$

$$304.92 * y = (300 * 5) + (3.16 * 2.375) + (1.76 * 7.875)$$

Upon solving $y = 4.99$ inches

$$I_g = \frac{30 * 1000}{12} + 1.76 * (2.875)^2 + 3.16 * (2.63)^2 = 2536 \text{ in}^4$$

$$M_{cr} = \frac{f_{ct} * I_g}{y} = \frac{7.5 \sqrt{4160}}{4.99 * 1000} * 2536 = 249.85 \text{ kip-inches} = 20.82 \text{ k-ft}$$

3.6.6.1 Calculation for Centroid and Moment of Inertia of Cracked Section (W1 & W2)

$$Y'^2 + \frac{2(n-1)A'_{st} + 2nA_s}{b} y' - \frac{2(n-1)A'_{st} + 2nA_{sd}}{b} = 0$$

Upon solving

$$Y' = 2.67 \text{ inches}$$

$$I_{cr} = b * y'^3 / 3 + (n-1) * A'_{st} * (y' - d')^2 + n * A_{st} * (d - y')^2$$

$$I_{cr} = 30 * (2.67)^3 / 3 + (6.88) * (1.76) * (2.67 - 2.125)^2 + (7.88 * 3.16) * (7.75 - 2.125)^2$$

$$I_{cr} = 836.72 \text{ in}^4$$

$$I_{eff} = I_g * (M_{cr} / M_a)^3 + I_{cr} * (1 - (M_{cr} / M_a)^3)$$

In above equation M_a is the actual moment at every loading stage.

Following formula can be used to compute theoretical deflection at every loading stage

$$\Delta_{max} = M_a * (3l^2 - 4a'^2) / 24E_{eff} I_{eff}$$

To take into account the effect of material non-linearity, E_{eff} is taken as $0.85E_c$

Where $E_c = 57\sqrt{f'} \text{ksi}$

Values of load and deflection at different loading stages are tabulated below

Total Load (Tons)	Maximum Deflection (mm)
0	0
4.54	1.87
9.07	3.83
13.6	8.22
18.14	12.24
22.68	15.96
27.22	19.53
31.76	23.02
36.29	26.45
40.83	29.86
45.37	32.26

Table 3.10 Theoretical Deflections of W1 & W2

W3 & W4

$$A_c = 300 \text{ in}^2$$

$$A_{st} = 6.32 \text{ in}^2$$

$$A'_{st} = 1.76 \text{ in}^2$$

$$A_T = 308.08 \text{ in}^2$$

$$308.08 * y = (300 * 5) + (6.32 * 2.375) + (1.76 * 7.75)$$

Upon solving $y = 4.96$ inches

$$I_g = \frac{30 * 1000}{12} + 1.76 * (2.79)^2 + 6.32 * (2.585)^2 = 2710 \text{ in}^4$$

$$M_{cr} = \frac{f_{ct} * I_g}{y} = \frac{7.5\sqrt{4160}}{4.96 * 1000} * 2710 = 264.29 \text{ kip-inches} = 22 \text{ k-ft}$$

3.6.6.2 Calculation for Centroid and Moment of Inertia of Cracked Section (W3 & W4)

$$Y'^2 + \frac{2(n-1)A'st+2nAs}{b}y' - \frac{2(n-1)A'st+2nAsd}{b} = 0$$

Upon solving

$$Y'=3.45 \text{ inches}$$

$$I_{cr} = b*y^3/3 + (n-1)*A'st*(y'-d)^2 + n*A_{st}*(d-y')^2$$

$$I_{cr} = 30*(3.45)^3/3 + (6.88)*(1.76)*(3.45-2.25)^2 + (7.88*6.32)*(7.625-2.25)^2$$

$$I_{cr} = 1296.14 \text{ in}^4$$

$$I_{eff} = I_g * (M_{cr}/M_a)^3 + I_{cr} * (1 - (M_{cr}/M_a)^3)$$

In above equation M_a is the actual moment at every loading stage.

Following formula can be used to compute theoretical deflection at every loading stage

$$\Delta_{max} = M_a * (3l^2 - 4a^2) / 24E_{eff} I_{eff}$$

To take into account the effect of material non-linearity, E_{eff} is taken as $0.85E_c$

$$\text{Where } E_c = 57\sqrt{f'} \text{ ksi}$$

Values of load and deflection at different loading stages are tabulated below

Total Load (Tons)	Maximum Deflection (mm)
0	0
4.54	1.02
9.07	2.84
13.61	5.58
18.14	8.03
22.68	10.33
27.22	12.56
31.76	14.75
36.29	16.92
40.83	19.09
45.37	21.23
49.91	23.38
54.44	25.52
59.89	28.1

Table 3.11 Theoretical Deflections of W3 & W4

M1 & M2

$$A_c = 400 \text{ in}^2$$

$$A_{st} = 3.95 \text{ in}^2$$

$$A'_{st} = 1.76 \text{ in}^2$$

$$A_T = 405.71 \text{ in}^2$$

$$405.71 * y = (400 * 5) + (3.95 * 2.25) + (1.76 * 7.875)$$

Upon solving $y = 4.985$ inches

$$I_g = \frac{40 * 1000}{12} + 1.76 * (2.89)^2 + 3.95 * (2.735)^2 = 3377.56 \text{ in}^4$$

$$M_{cr} = \frac{f_{ct} * I_g}{y} = \frac{7.5 \sqrt{4160}}{4.985 * 1000} * 3377.56 = 327.75 \text{ kip-inches} = 27.31 \text{ k-ft}$$

3.6.6.3 Calculation for Centroid and Moment of Inertia of Cracked Section (M1 & M2)

$$Y'^2 + \frac{2(n-1)A'st+2nAs}{b}y' - \frac{2(n-1)A'st+2nAsd}{b} = 0$$

Upon solving

$$Y'=2.55 \text{ inches}$$

$$I_{cr} = b*y^3/3 + (n-1)*A'st*(y'-d)^2 + n*A_{st}*(d-y')^2$$

$$I_{cr} = 40*(2.55)^3/3 + (6.88)*(1.76)*(2.55-2.125)^2 + (7.88*3.95)*(7.75-2.125)^2$$

$$I_{cr} = 1208.11 \text{ in}^4$$

$$I_{eff} = I_g * (M_{cr}/M_a)^3 + I_{cr} * (1-(M_{cr}/M_a)^3)$$

In above equation M_a is the actual moment at every loading stage.

Following formula can be used to compute theoretical deflection at every loading stage

$$\Delta_{max} = M_a * (3l^2 - 4a'^2)/24E_{eff} I_{eff}$$

To take into account the effect of material non-linearity, E_{eff} is taken as $0.85E_c$

$$\text{Where } E_c = 57\sqrt{f'} \text{ ksi}$$

Values of load and deflection at different loading stages are tabulated below

Total Load (Tons)	Maximum Deflection (mm)
0	0
4.54	0.82
9.07	1.86
13.61	4.82
18.14	7.81
22.68	10.57
27.22	13.17
31.76	15.67
36.29	18.12
40.83	20.52
45.37	22.90
49.91	25.26
54.44	27.61

Table 3.12 Theoretical Deflections of M1 & M2

M3 & M4

$$A_c = 400 \text{ in}^2$$

$$A_{st} = 7.9 \text{ in}^2$$

$$A'_{st} = 1.76 \text{ in}^2$$

$$A_T = 409.66 \text{ in}^2$$

$$409.66 * y = (400 * 5) + (7.9 * 2.375) + (1.76 * 7.75)$$

Upon solving $y = 4.96$ inches

$$I_g = \frac{40 * 1000}{12} + 1.76 * (2.79)^2 + 7.9 * (2.585)^2 = 3400 \text{ in}^4$$

$$M_{cr} = \frac{f_{ct} * I_g}{y} = \frac{7.5 \sqrt{4160}}{4.96 * 1000} * 3400 = 331.59 \text{ kip-inches} = 27.63 \text{ k-ft}$$

3.6.6.4 Calculation for Centroid and Moment of Inertia of Cracked Section (M3 & M4)

$$Y'^2 + \frac{2(n-1)A'_{st} + 2nA_s}{b} y' - \frac{2(n-1)A'_{st} + 2nA_{sd}}{b} = 0$$

Upon solving

$$Y' = 3.413 \text{ inches}$$

$$I_{cr} = b * y'^3 / 3 + (n-1) * A'_{st} * (y' - d')^2 + n * A_{st} * (d - y')^2$$

$$I_{cr} = 40 * (3.413)^3 / 3 + (6.88) * (1.76) * (3.413 - 2.25)^2 + (7.88 * 7.9) * (7.625 - 2.25)^2$$

$$I_{cr} = 1650.79 \text{ in}^4$$

$$I_{eff} = I_g * (M_{cr} / M_a)^3 + I_{cr} * (1 - (M_{cr} / M_a)^3)$$

In above equation M_a is the actual moment at every loading stage.

Following formula can be used to compute theoretical deflection at every loading stage

$$\Delta_{max} = M_a * (3l^2 - 4a^2) / 24 E_{eff} I_{eff}$$

To take into account the effect of material non-linearity, E_{eff} is taken as $0.85 E_c$

$$\text{Where } E_c = 57 \sqrt{f'} \text{ ksi}$$

Values of load and deflection at different loading stages are tabulated below

Total Load (Tons)	Maximum Deflection (mm)
0	0
4.54	0.81
9.07	1.71
13.61	3.91
18.14	5.98
22.68	7.88
27.22	9.7
31.76	11.46
36.29	13.19
40.83	14.91
45.37	16.61
49.91	18.31
54.44	20.00
58.98	21.68
63.52	23.37
68.05	25.05
72.56	26.74
77.13	28.41
81.67	30.09

Table 3.13 Theoretical Deflections of M3 & M4

Chapter -4

EXPERIMENTAL RESULTS

4.1 Concrete Strength

Twelve cubes of 6" x 6" were made at the time of pouring and casting of beams. Cubes were tested at the age of 7, 14, 28 days. 2 cubes were tested at the day of testing of beams. The average compressive cylinder strength derived from cube strength came out to be 4160 psi.

4.2 Testing Setup

Four point bending method was adopted for testing of beams. A rigid steel girder was used to convert the single load into two point loads. Two steel plates were placed below the girder for transfer of load from steel girder to the beam to be tested. An a'/d ratio of 4.5 was maintained for all beams to provide a shear span which would depict behavior of a uniformly loaded beam. Test arrangements are shown in the figure below



Fig4.1 Testing Setup

4.3 Measurements

4.3.1 Deflections

Three electronic LVDTs were installed, one below mid span and remaining two below middle third of the beam. LVDTs were calibrated to zero before application of load on beam. Load was applied at an interval of 3 tons. Values of deflection at each load were recorded in the computer.

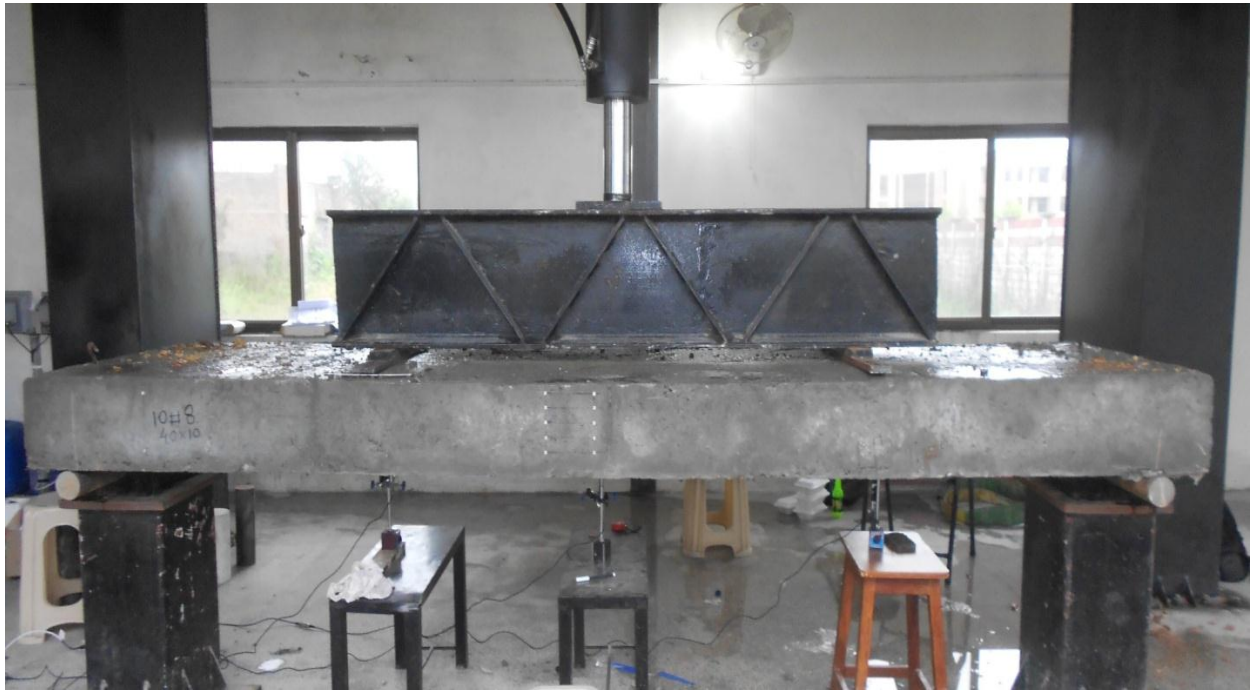


Fig4.2 Testing Setup showing LVDTs

4.3.2 Strains

An attempt was made to measure the longitudinal strains with the help of demic points manually. Demic points were attached on the surface of beam on its side with the help of adhesive. These points were attached 1.5” apart vertically and 6” apart horizontally. Portion of span of beam between point loads was supposed to have constant moment therefore, Demic points were attached at middle span of the beam. The aim was to establish a strain profile across the depth of the beam with the help of measured strains. Multi position strain gauge was used to measure

longitudinal strains. At every load increment reading of gauge was noted down manually. Figure 4.3 shows the demic points attached across the depth of the beam



Fig4.3 Demic points attached across the depth

4.4 Test Behavior of Specimens

All beams were tested at NUST Laboratory on 31st march, 2015. Load was applied gradually with an interval of 3 tons. Initiation, Propagation and widening of cracks were marked at corresponding loads at different stages. Detailed behavior of each beam is as below:-

4.4.1 Specimen W-1

Initial flexural cracks appeared at a load of 10 tons under the loading point. Deflection of beam reached ACI maximum permissible deflection limit at a load of 14 tons. At a load of 22 tons flexural cracks also appeared in the middle span of the beam. As load was increasing the cracks became wider. Flexure cracks became inclined because of shear at a load of 30 tons. Beam behaved as a Tension controlled one because the deflection kept on increasing with increase of load. Ultimate failure happened at a load 45 tons by crushing of concrete in compression zone on top of beam. Failure occurred with a sharp sound. Ultimate failure was a type of sudden failure

but overall behavior can be regarded as ductile behavior as the beam deflected up to 45mm and no web shear cracks appeared during whole loading period. Cracking pattern is shown in figure 4.4. Deflected shape of the beam at different load stages is shown in figure 4.5. Figure 4.6 shows the load versus deflection curve of W1.



Fig4.4 Cracking pattern of W1

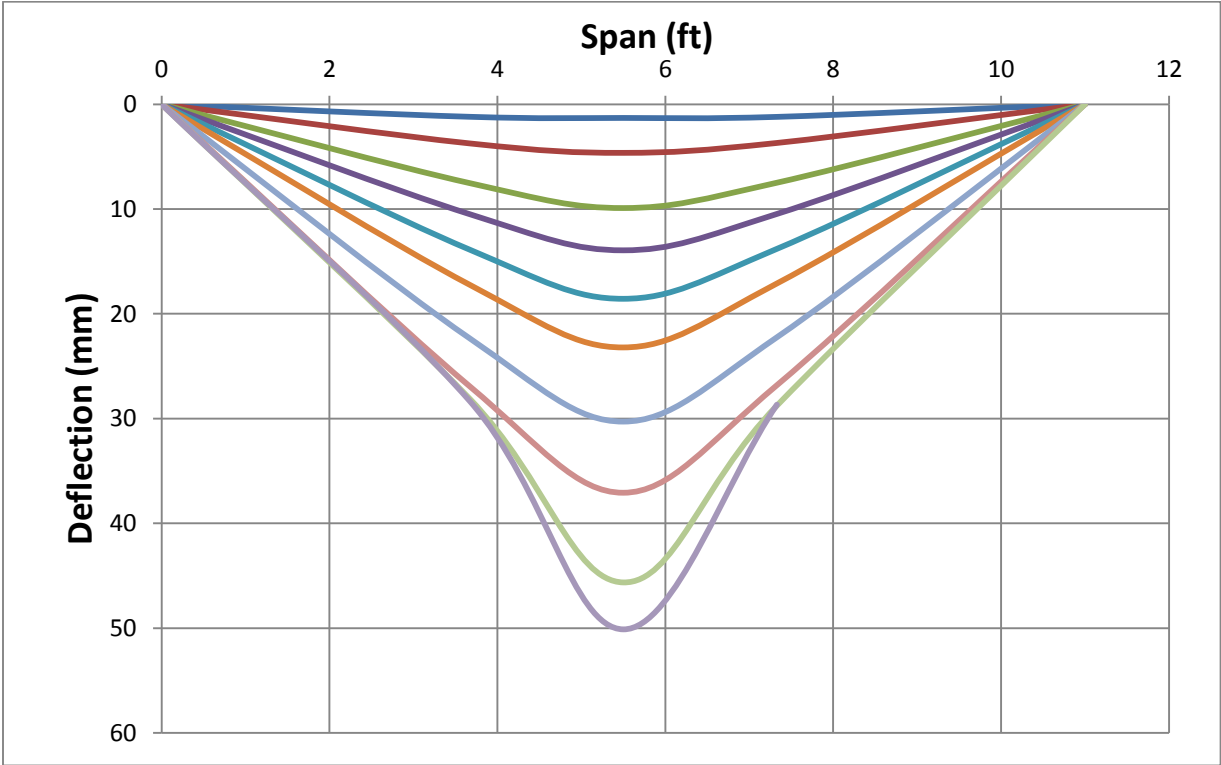


Fig4.5 Deflected Shape of W1

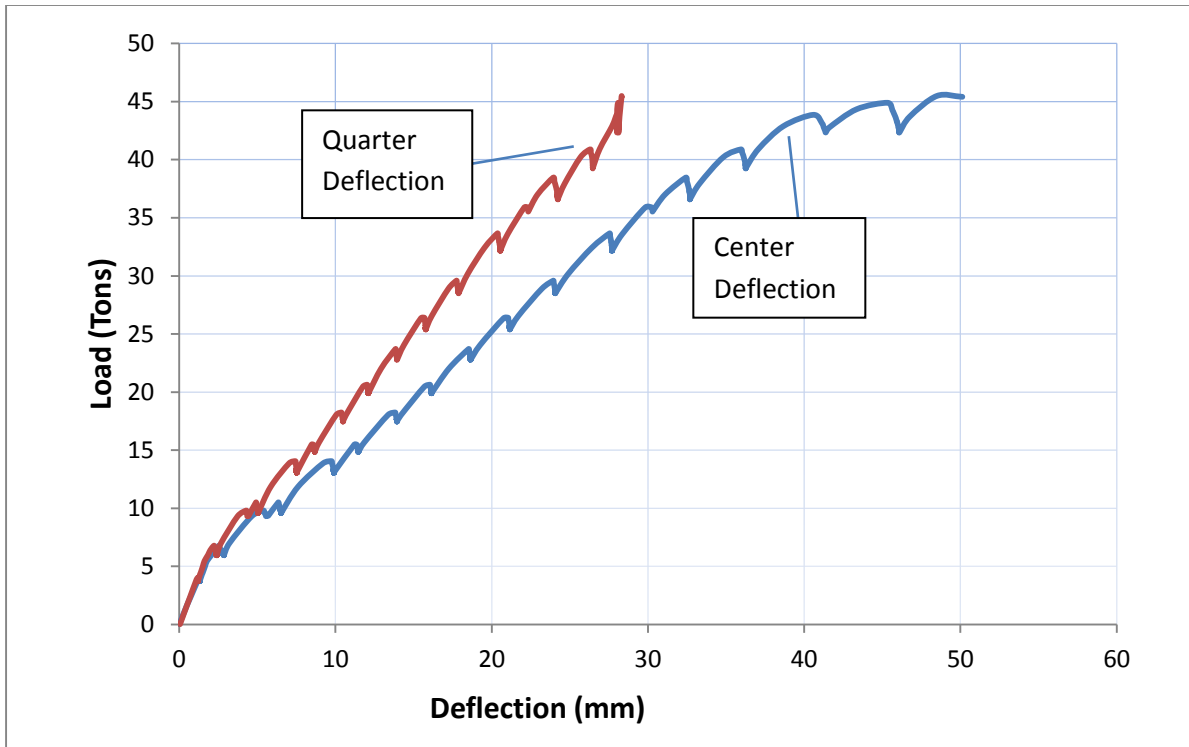


Fig4.6 Load vs Deflection Curve of W1

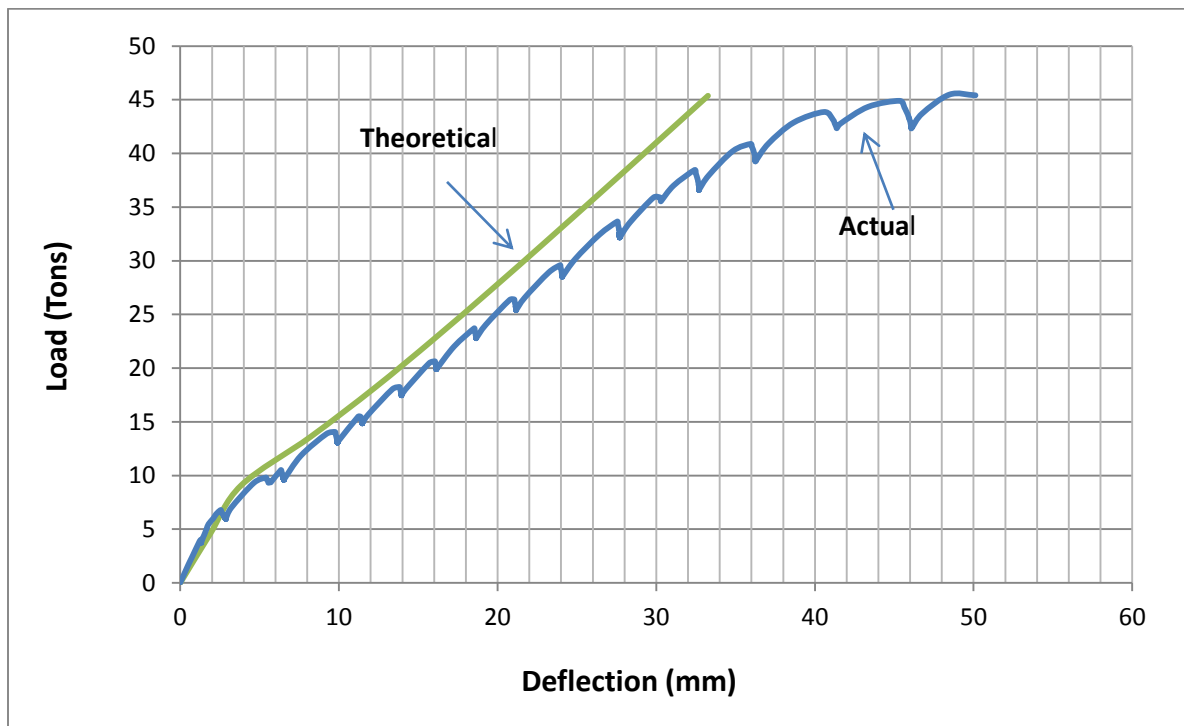


Fig. 4.7 theoretical versus actual deflections of W1

4.4.2 Specimen W-2

Initial flexural cracks appeared at a load of 12 tons in the middle span i.e. between the two loading points. Deflection of beam reached ACI maximum permissible deflection limit at a load of 15 tons. Number of flexural cracks increased in the middle span of the beam at a load of 28 tons. As load was increasing the cracks became wider. At a load of 30 tons flexure cracks became inclined because of shear. Beam behaved as a tension controlled one because it achieved the design moment capacity without any shear or compression failure. Ultimate failure occurred at a load of 45 tons and load value on the data recording computer started decreasing with further increase of load from the loading machine. Cracking pattern is shown in figure 4.7. Figure 4.8 shows the load versus deflection curve of W2. Deflected shape of the beam at different load stages is shown in figure 4.9.



Fig4.8 Cracking pattern of W2

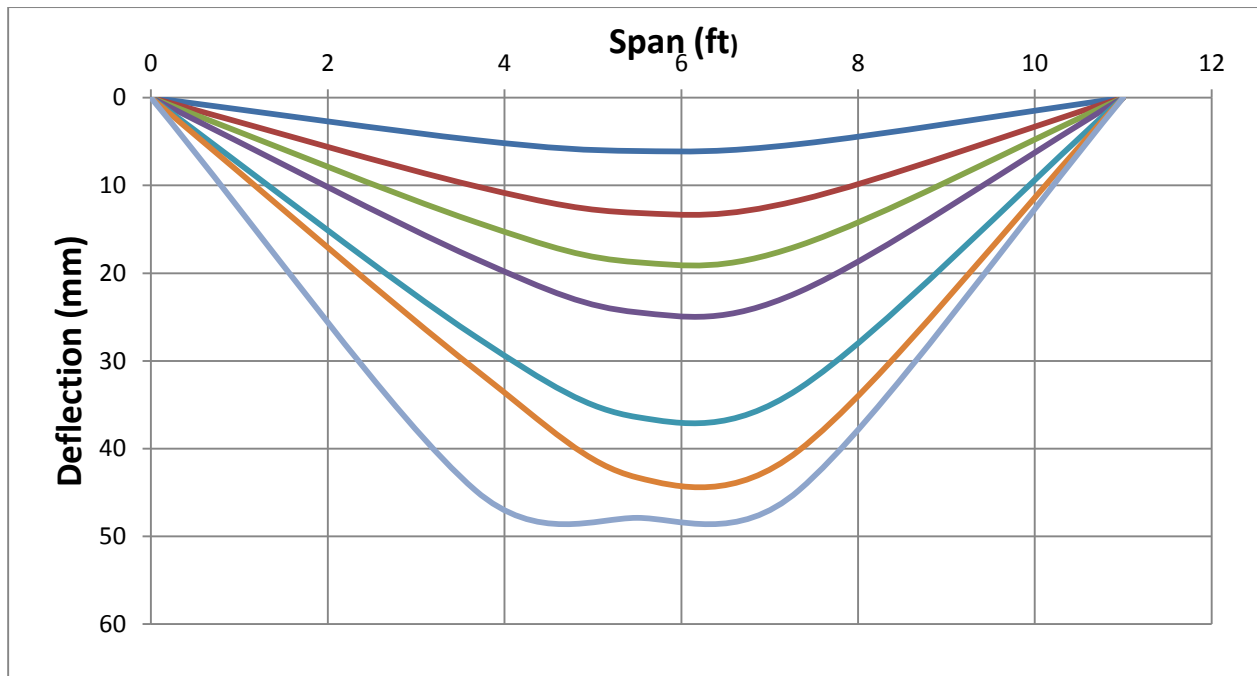


Fig4.9 Load vs Deflection Curve of W2

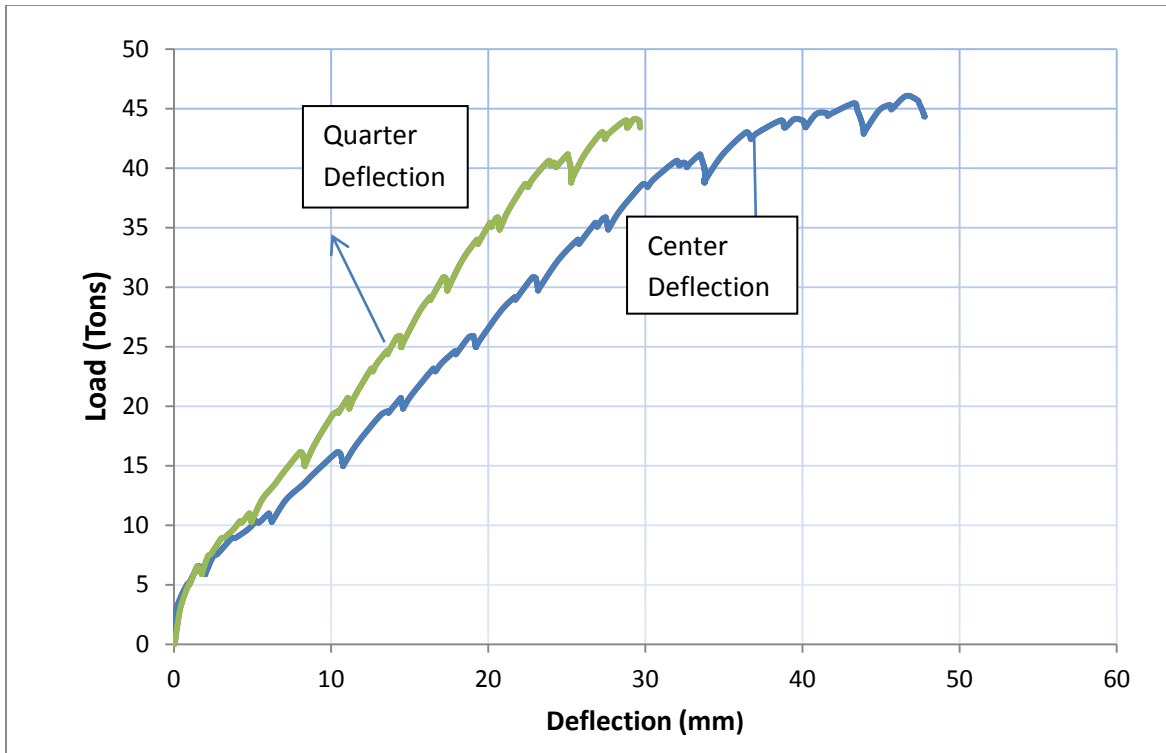


Fig4.10 Deflected Shape of W2

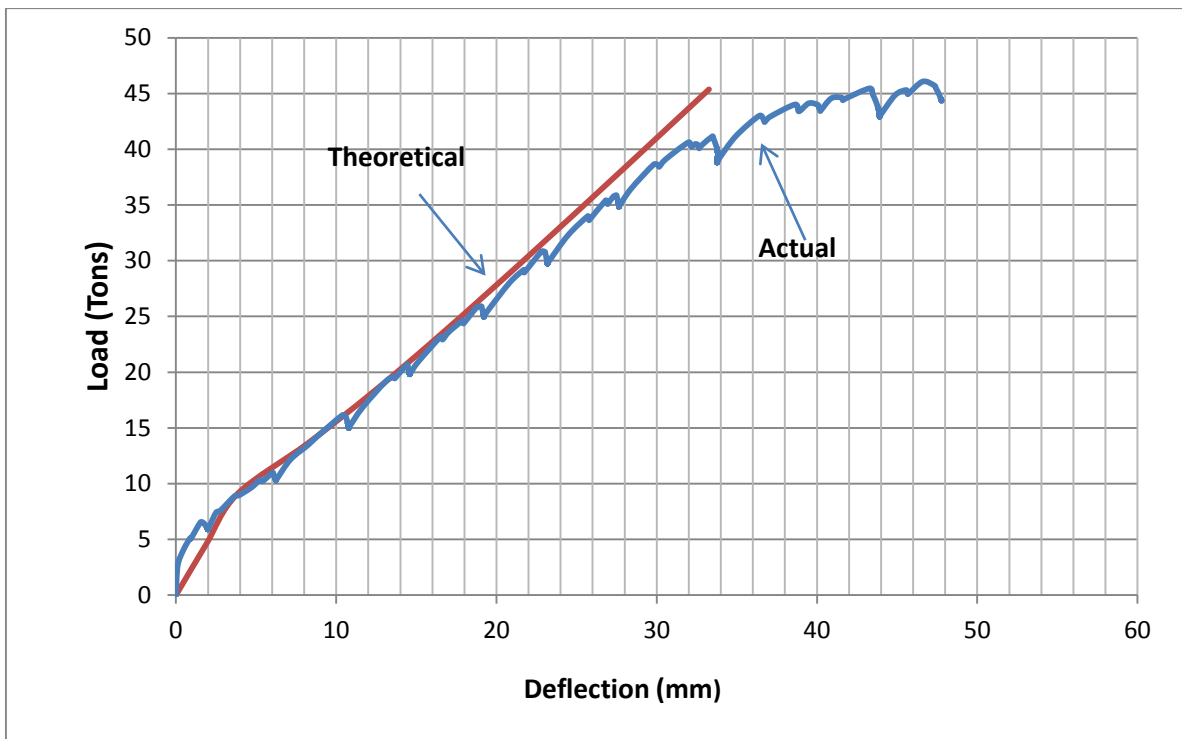


Fig. 4.11 theoretical versus actual deflections of W2

4.4.3 Specimen W-3

Initial flexural cracks appeared in the middle third span of the beam at a load of 12 tons. Deflection of beam reached ACI maximum permissible deflection limit at a load of 23 tons. Cracks became wider at a load of 28 tons and penetrated into half of the beam depth till a load of 40 tons. First Shear cracks appeared at a load of 53 tons on both sides near the support. First branch of Shear cracks appeared at a distance of 11 inches from the center of support. As the load was increased to 58 tons, another branch of cracks was observed near the first branch. Upon further increase of load the shear cracks entered the compression zone causing a shear compression failure. There was a sharp sound at the time of failure. Almost horizontal cracks at the level of tension steel, moving from shear crack towards the support were also observed at the time of failure representing anchorage failure. Cracking pattern of the specimen W3 is shown in figure 4.10. Figure 4.12 shows the load versus deflection curve of specimen W3 while deflected shape of this beam is shown in figure 4.13.



Fig4.12 Cracking Pattern of W3



Fig4.13 Picture showing distance of shear crack from center of support

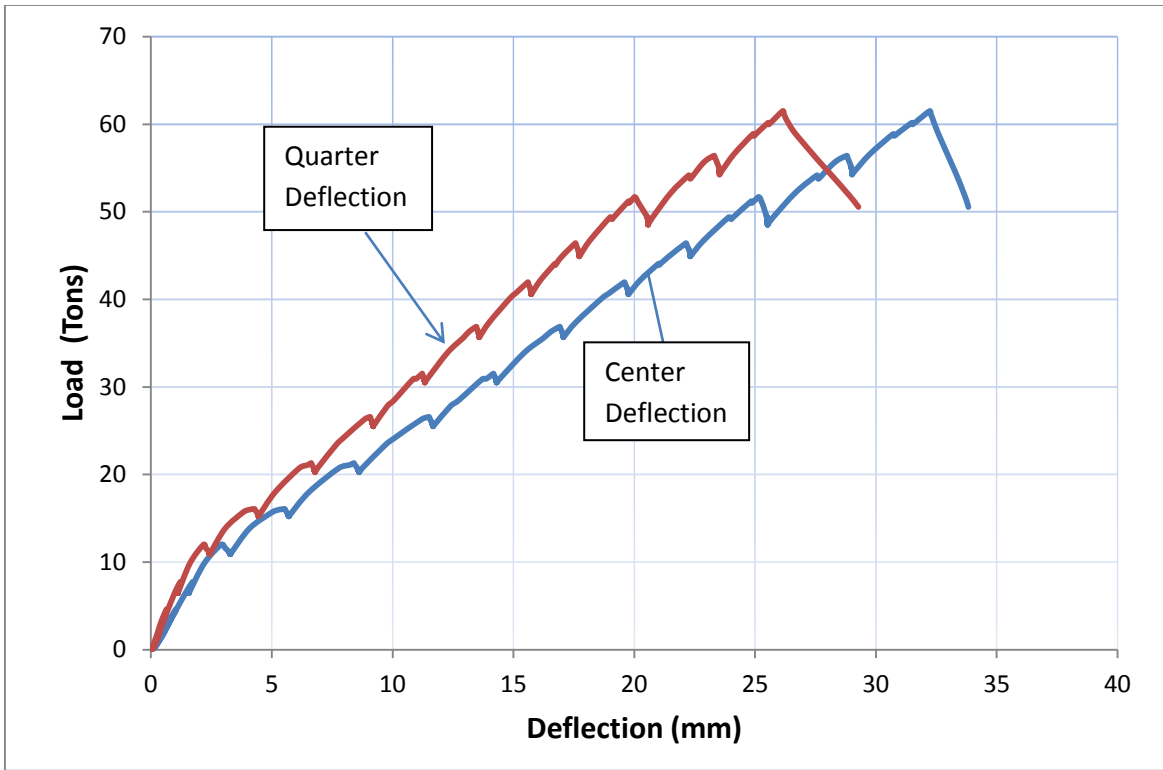


Fig4.14 Load vs Deflection Curve of W3

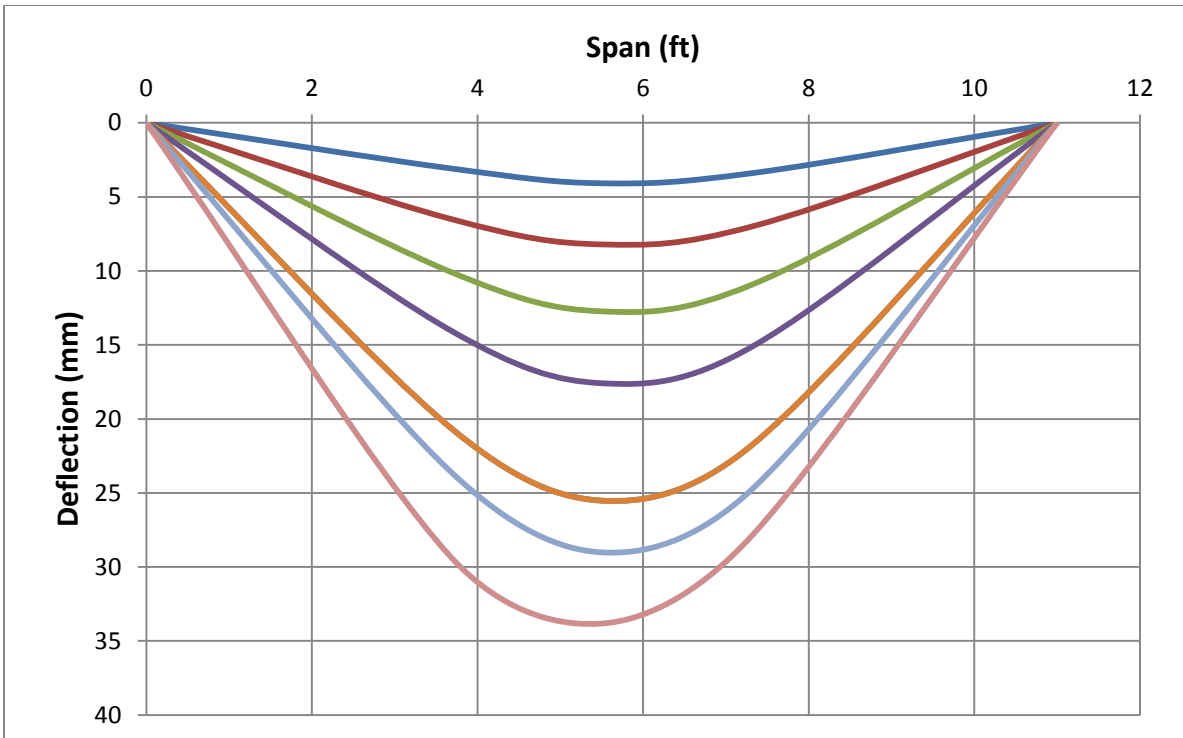


Fig.4.15 Deflected Shape of W3

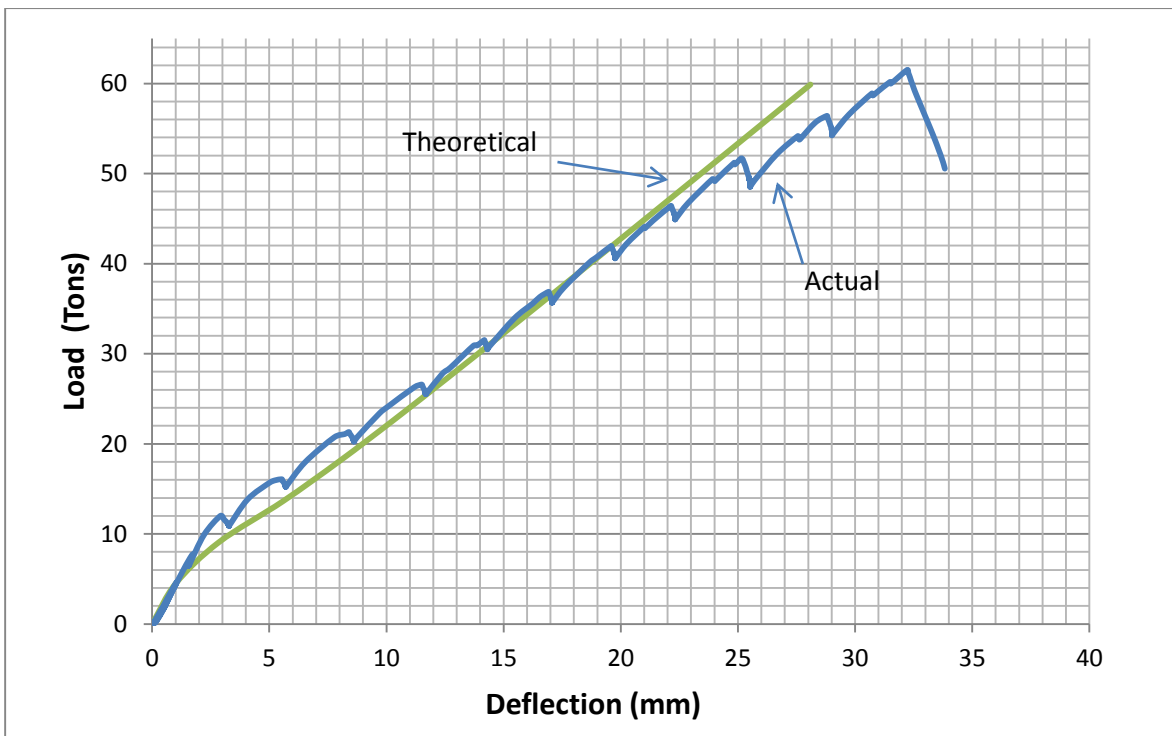


Fig. 4.16 theoretical versus actual deflections of W3

4.4.4 Specimen W-4

Initial flexural cracks appeared in the middle third span of the beam at a load of 11 tons. Deflection of beam reached ACI maximum permissible deflection limit at a load of 24 tons. Cracks became wider at a load of 35 tons and penetrated into half of the beam depth till a load of 40 tons. First Shear cracks appeared at a load of 53 tons on both sides near the support. First branch of Shear cracks appeared at a distance of 11 inches from the center of support. As the load was increased to 57 tons, another branch of cracks was observed near the first branch. Upon further increase of load the shear cracks entered the compression zone causing a shear compression failure. There was a sharp sound at the time of failure. Almost horizontal cracks at the level of tension steel, moving from shear crack towards the support were also observed at the time of failure representing anchorage failure. Cracking pattern of the specimen W4 is shown in figure 4.14. Figure 4.15 shows the load versus deflection curve of specimen W4 while deflected shape of this beam is shown in figure 4.14.



Fig4.17 Cracking Pattern of W4

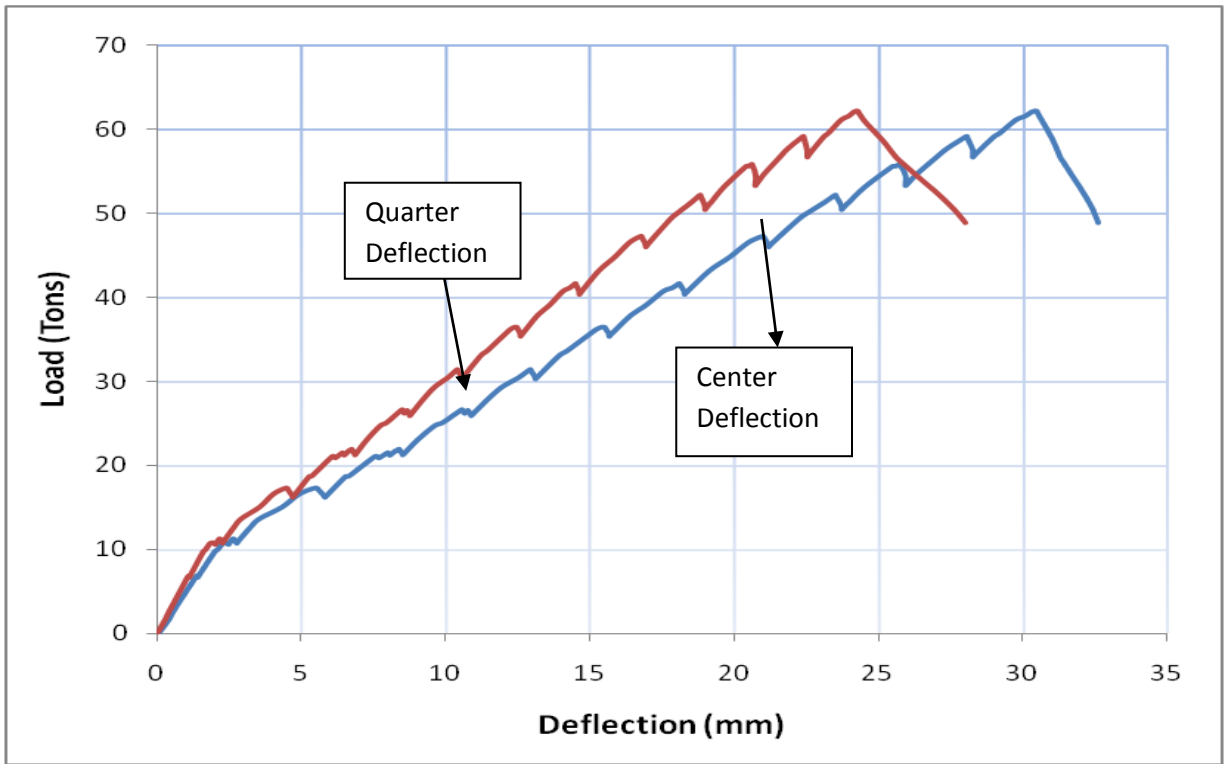


Fig.4.18 Load vs Deflection Curve of W4

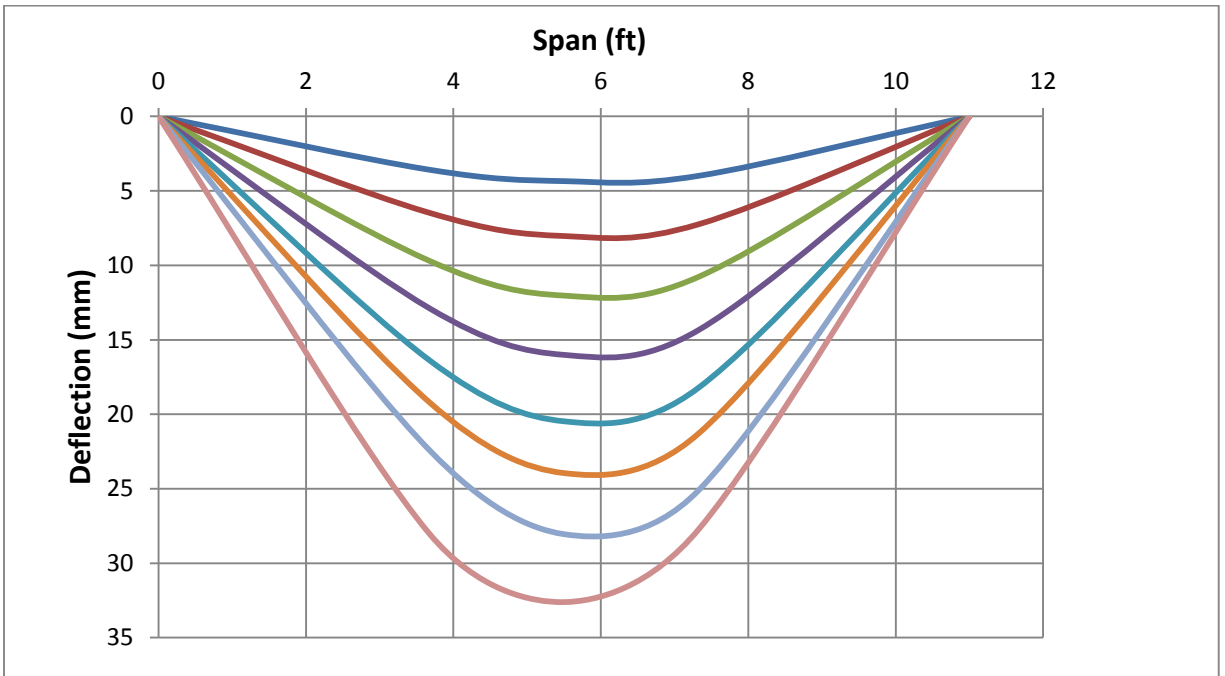


Fig.4.19 Deflected Shape of W4

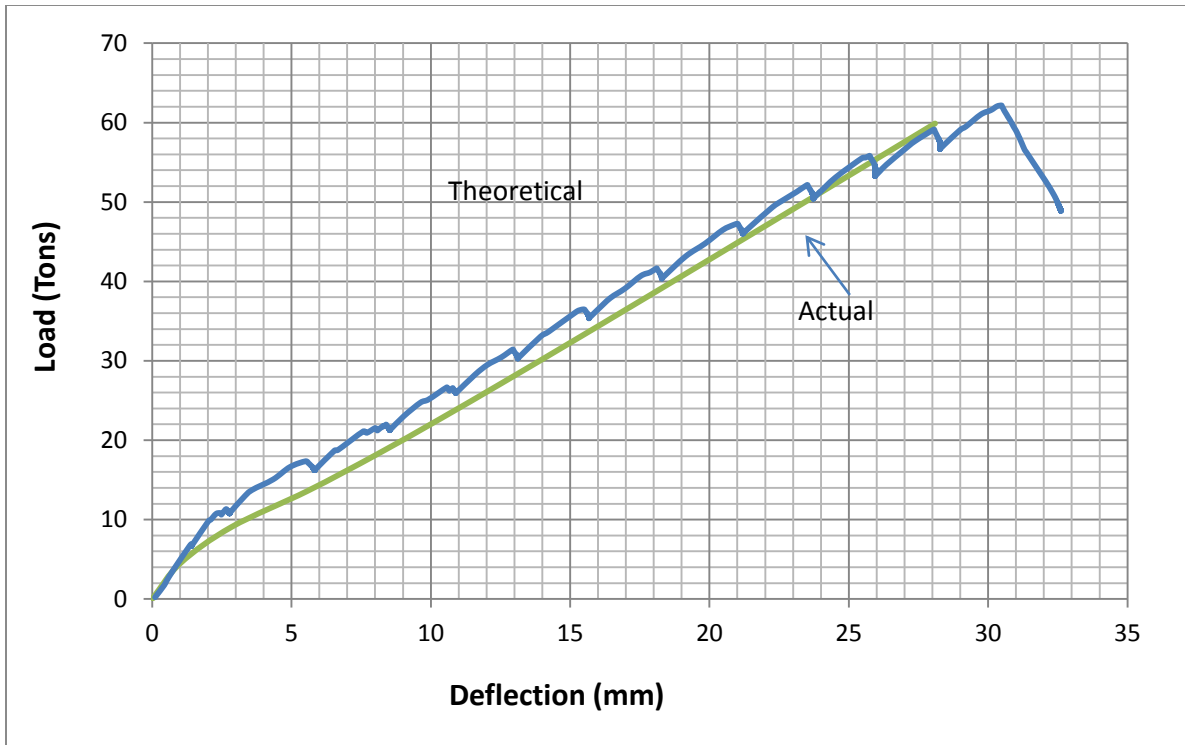


Fig. 4.20 theoretical versus actual deflections of W4

4.4.5 Specimen M-1

Hairline flexural cracks appeared at a load of 14 tons in middle span of the beam. Deflection of beam reached ACI maximum permissible deflection limit at a load of 18 tons. Flexural Cracks became wider at a load of 20 tons. It was observed that beam behaved in a ductile manner. Flexural cracks in shear span region started bending into compression zone ending up into flexure shear cracks. At a deflection of 48mm the load stopped to increase rapidly. Any further attempt to increase the load resulted in larger deflection but the load reading remained stable at 53 tons. Figure 4.16 shows the cracking pattern of W5. Load versus deflection curve is shown in the figure 4.17 and deflected shape of beam is shown in figure 4.18

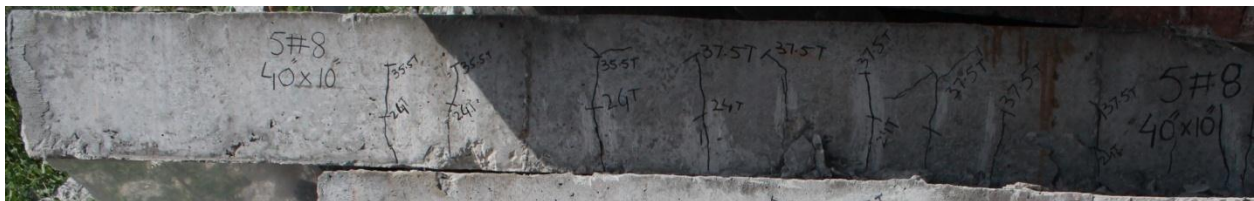


Fig4.21 Cracking Pattern of M1

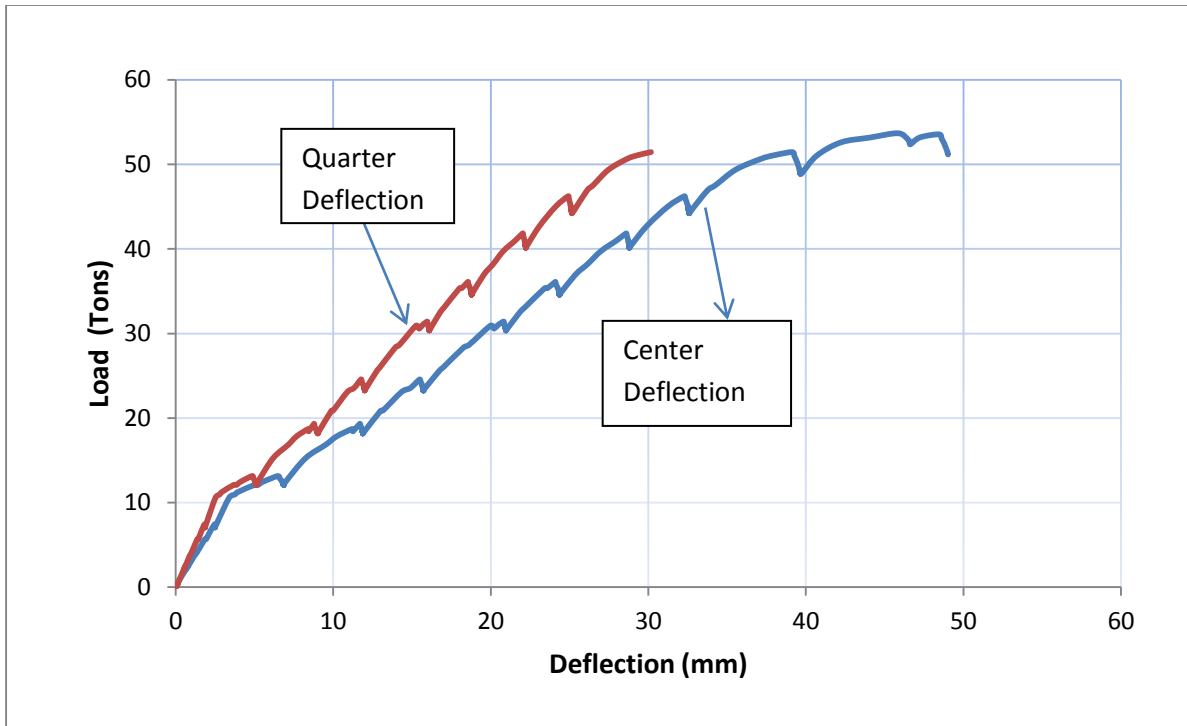


Fig4.22 Load vs Deflection Curve of M1

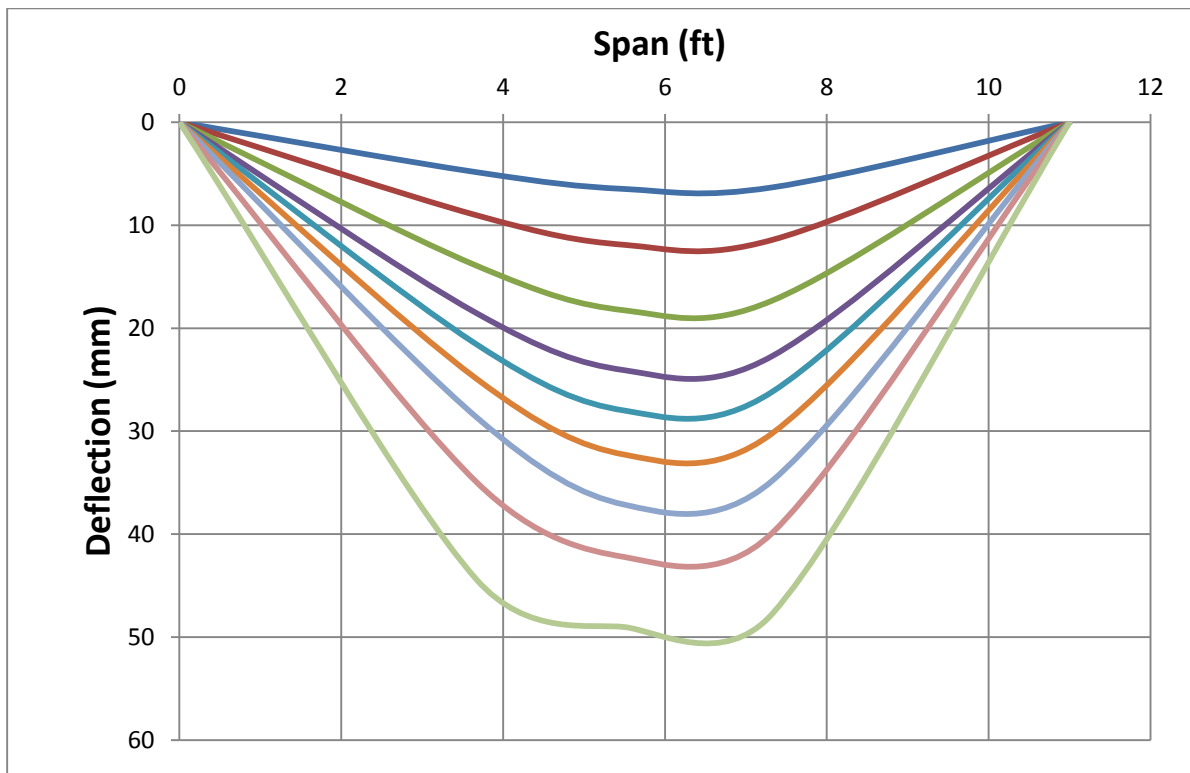


Fig4.23 Deflected Shape of M1

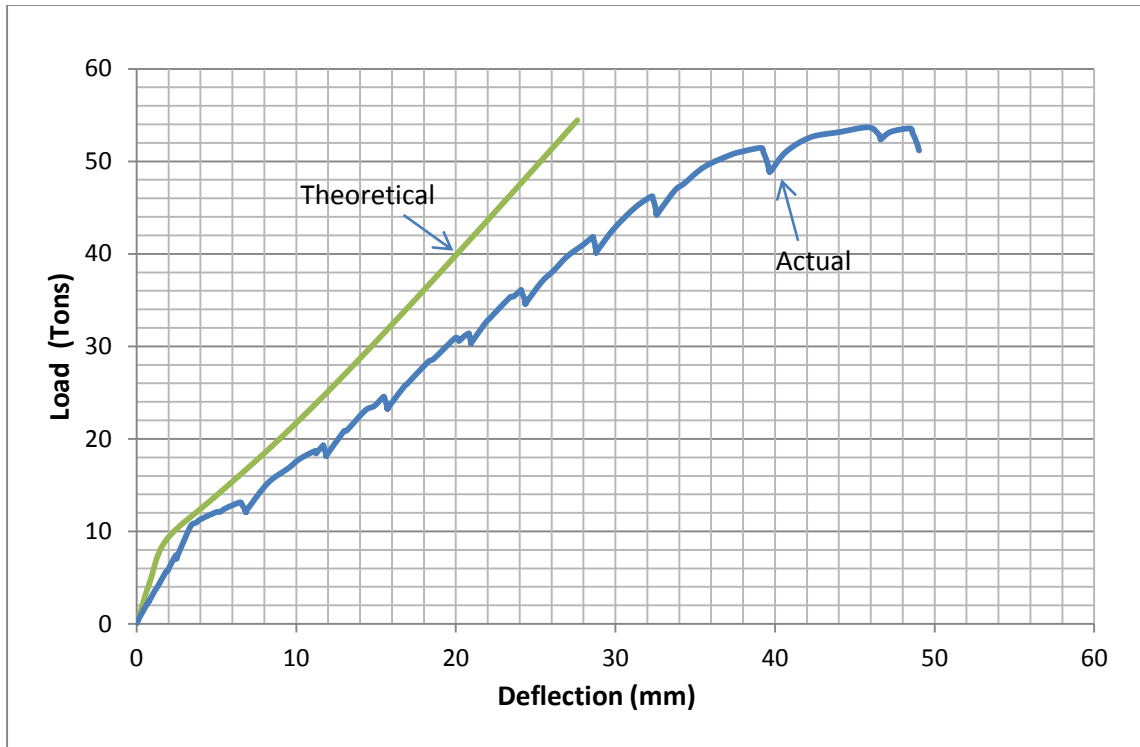


Fig. 4.24 theoretical versus actual deflections of **M1**

4.4.6 Specimen M-2

Flexural cracks appeared in middle span of the beam at a load of 10 tons. Deflection of beam reached ACI maximum permissible deflection limit at a load of 16 tons. Flexural cracks remained vertical up to a load of 18 tons. At 47 tons the flexural cracks bent into the compression zone and became flexure shear cracks. Shear cracks also appeared between the loading point and support at a load of 28 tons. Further increase of load widened the existing flexure and shear cracks. Failure occurred at a maximum deflection of 47mm. Flexure failure was observed at a load of 36 tons. Above this load beam was deflecting but load was not increasing. Cracking pattern is shown in figure 4.19. Load versus deflection graph is shown in figure 4.20. Deflected shape is shown in figure 4.21.



Fig4.25 Cracking Pattern of M2

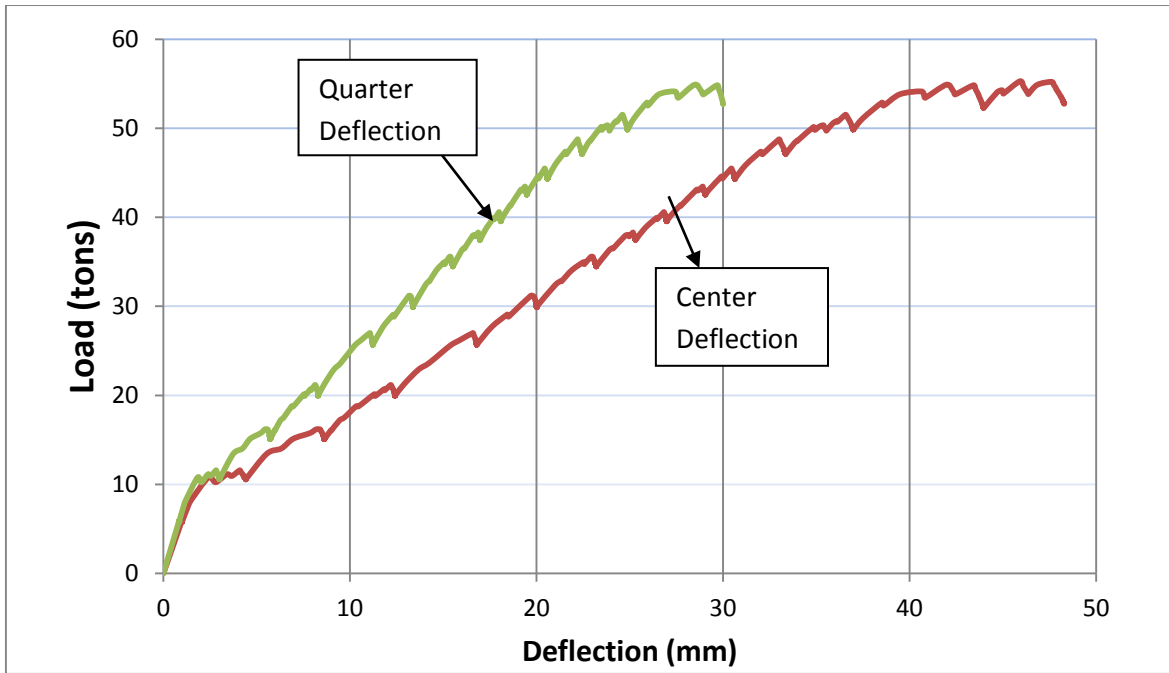


Fig4.26 Load vs Deflection Curve of M2

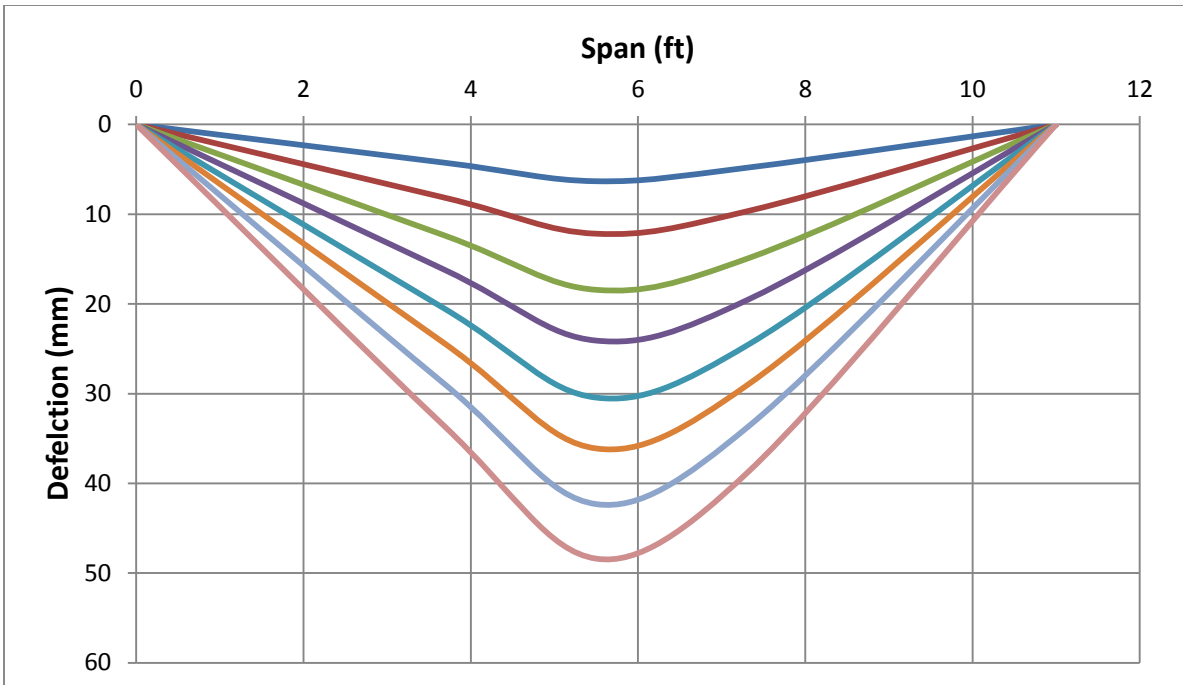


Fig 4.27 Deflected Shape of M2

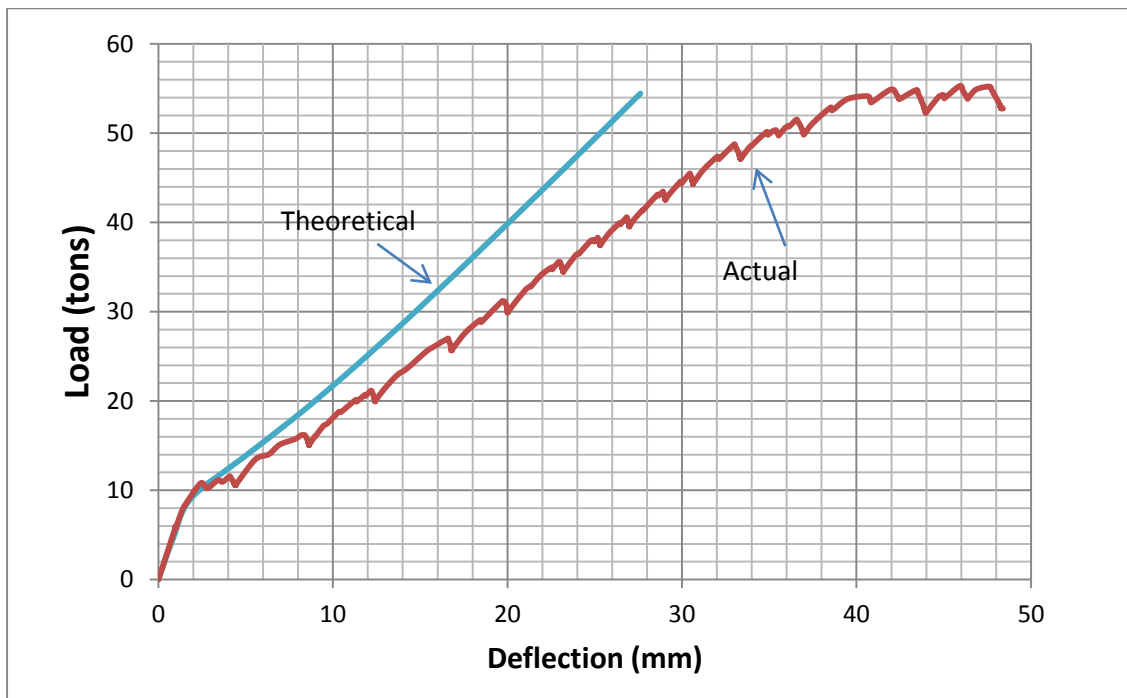


Fig. 4.28 theoretical versus actual deflections of M2

4.4.7 Specimen M-3

Initial flexural cracks appeared at a load of 22 tons. It was observed that deflection reached the maximum ACI permissible deflection limit at a load of 25 tons. Flexural cracks did not penetrate much into the depth of the beam but upon further increase of load, shear cracks started appearing between the load and support. First shear crack appeared at a load of 50 tons. When load was further increased the shear cracks went inclined in the compression zone. From 50 to 60 tons these shear cracks widened and sudden shear failure with a sharp sound happened at a load of 60 tons. Cracking pattern of the beam is shown in figure 4.22. Load versus deflection curve is shown in figure 4.23. Deflected shape of beam is shown in figure 4.24.



Fig4.29 Cracking Pattern of M3

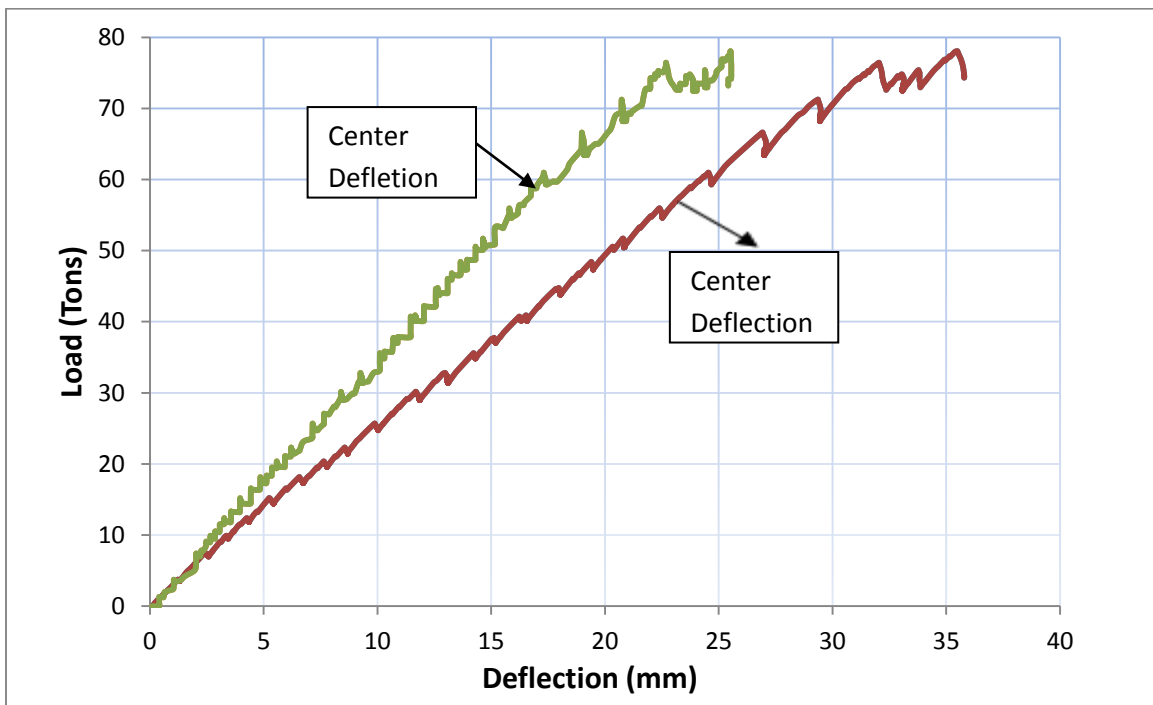


Fig4.30 Load vs Deflection Curve of M3

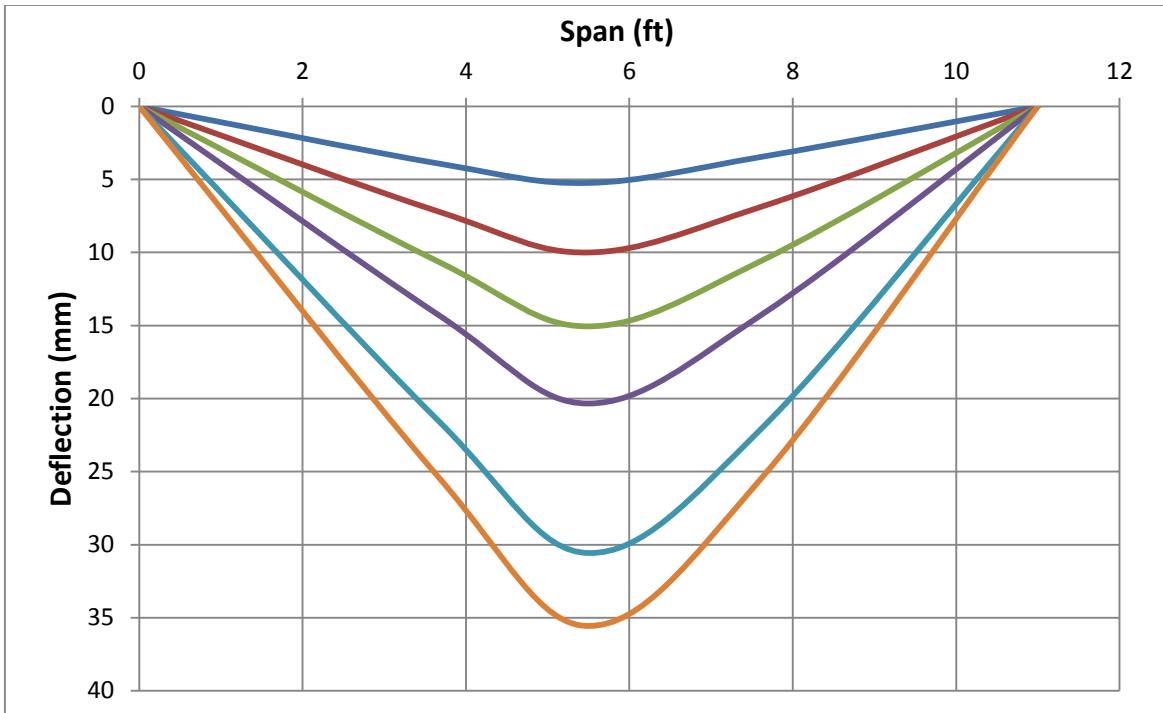


Fig 4.31 Deflected Shape of M3

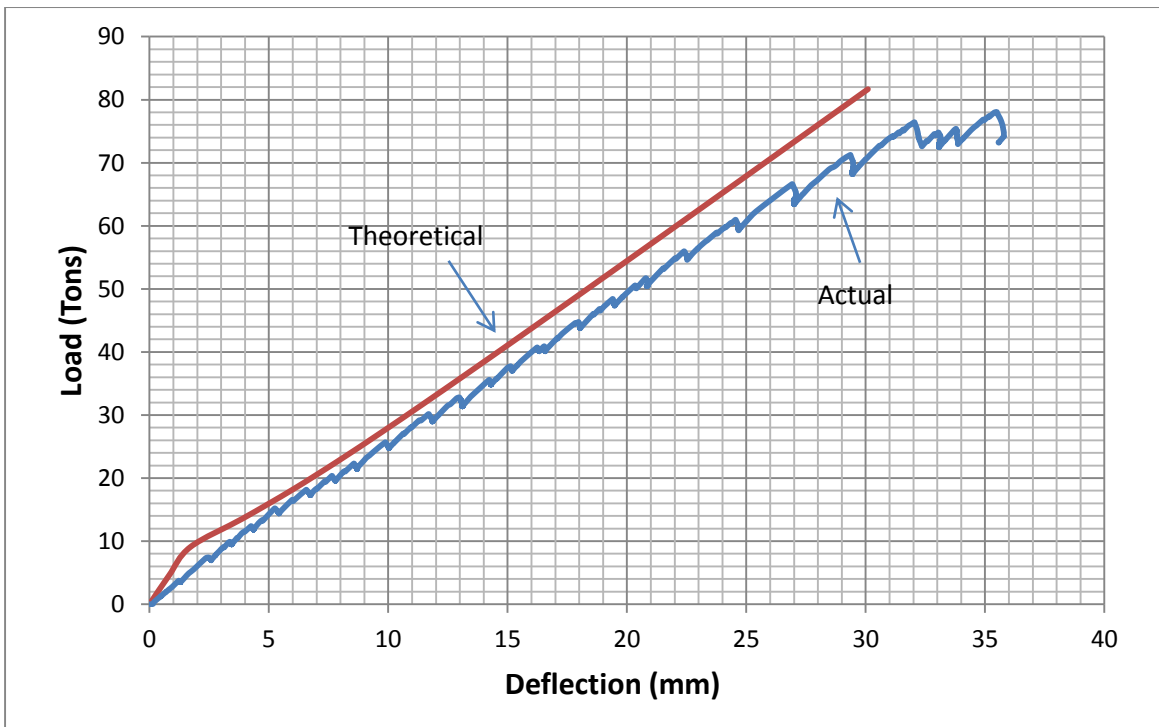


Fig. 4.32 theoretical versus actual deflections of M3

4.4.8 Specimen M-4

Initial flexural cracks appeared at a load of 24 tons. Deflection reached the maximum ACI permissible deflection limit at a load of 28 tons. Flexural cracks did not penetrate much into compression zone of the beam. Upon further increase of load, shear cracks started appearing between the load and support. First shear crack appeared at a load of 47 tons. When load was further increased the shear cracks went inclined in the compression zone. From 50 to 63 tons these shear cracks widened and sudden shear failure with a sharp sound happened at a load of 60 tons. Cracking pattern of the beam is shown in figure 4.25. Load versus deflection curve is shown in figure 4.26. Deflected shape of beam is shown in figure 4.27.



Fig4.33 Cracking Pattern of M4

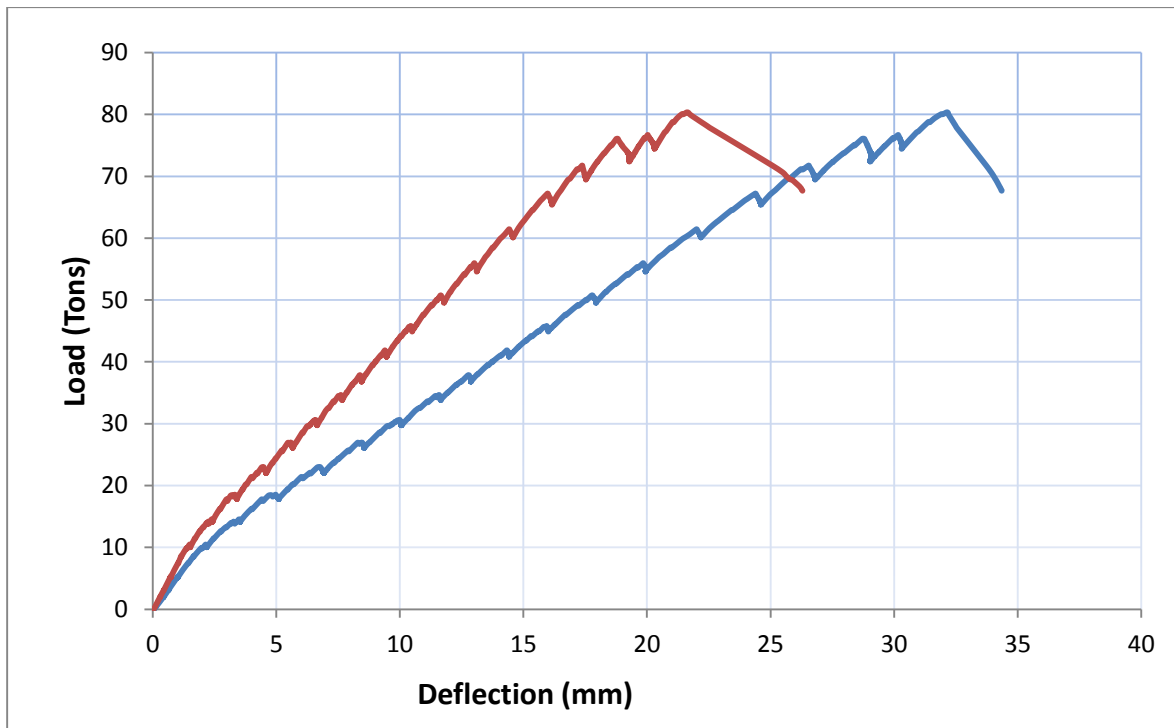


Fig4.34 Load vs Deflection Curve of M4

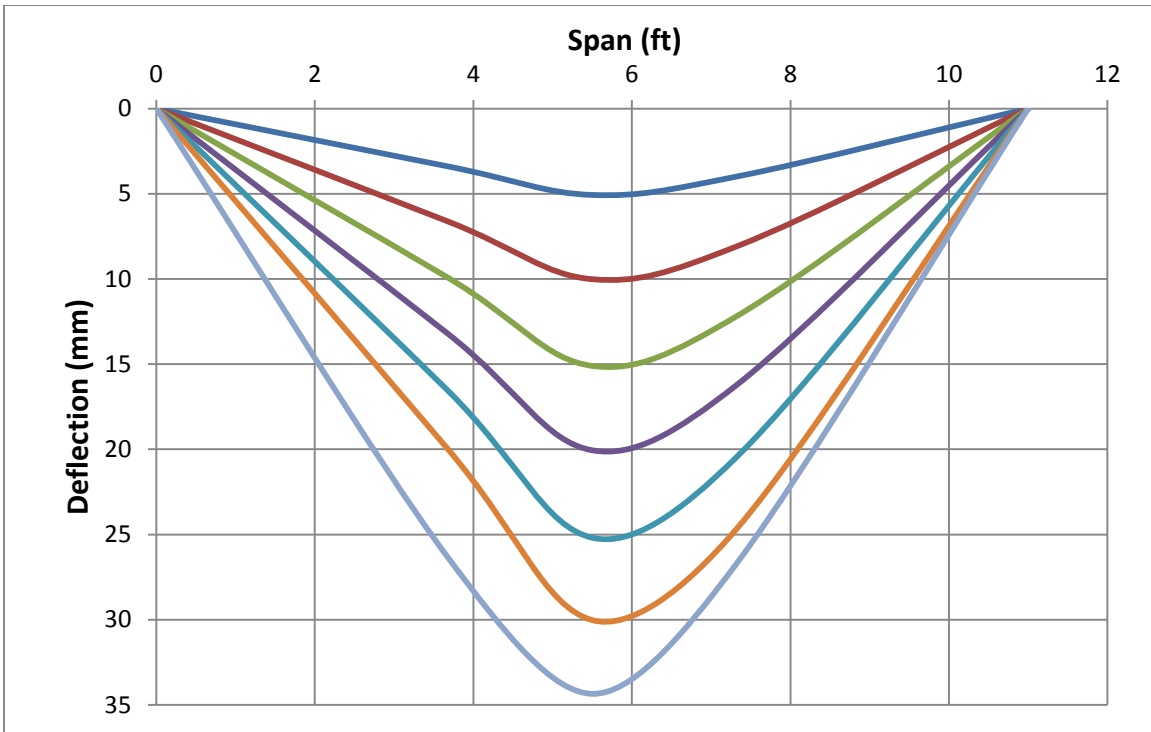


Fig4.35 Deflected Shape of M4

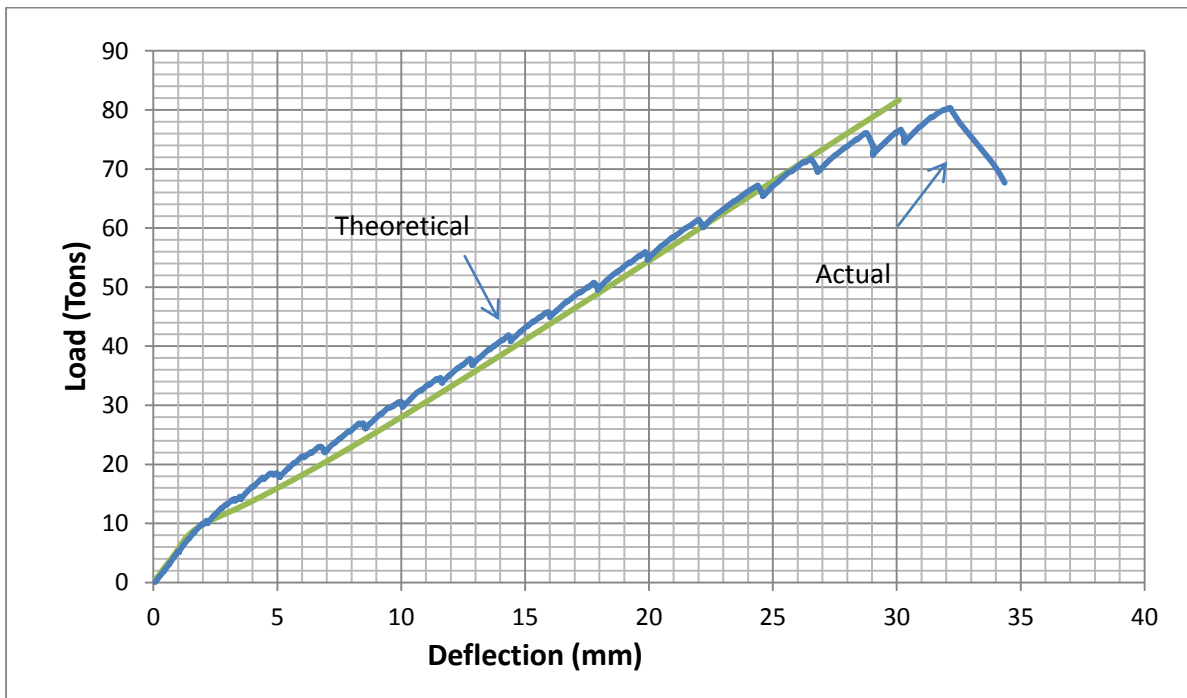


Fig. 4.36 theoretical versus actual deflections of M4

4.5 Summary of Test Results

Behavior of all beams can be summarized as below:

4.5.1 W1, W2, M1 and M2

These beams had comparable reinforcement ratio and behaved as true tension controlled members. No shear or compression failure was observed in these beams. Initiation of flexural cracks for these ductile beams started between 12 – 15 tons load. Flexural Cracks became wider with the increments of load and moved towards the compression zone. Before failure these beams behaved in a ductile manner. Failure of these beams was recognized from the observation that at failure the load reading became stable and it did not increase rather decreased by applying next increment. Moment capacity achieved was 15% and 16% more than the theoretical for W1 and W2 respectively while M1 and M1 achieved 10% and 8% increased moment capacity.

4.5.2 W3, W4, M3 and M4

These beams had comparable longitudinal reinforcement ratio, 0.0276 for W3 and W4 and 0.0259 for M3 and M4. Ultimate failure was shear compression failure. Beams took higher loads at comparatively lower deflections. Flexural cracks became visible between 18-22 tons load. Penetration and widening of flexural cracks was not significant. W3, W4, M3 and M4 just achieved their designed moment capacities. Upon increasing load, Instead of widening and penetration of flexural cracks the shear cracks became wider and penetrated into compression zone. Sudden shear compression failure occurred at ultimate loads. Inclination of shear cracks was measured between 30-45 degrees. Combined behavior of all beams can be seen in figure 4.37.

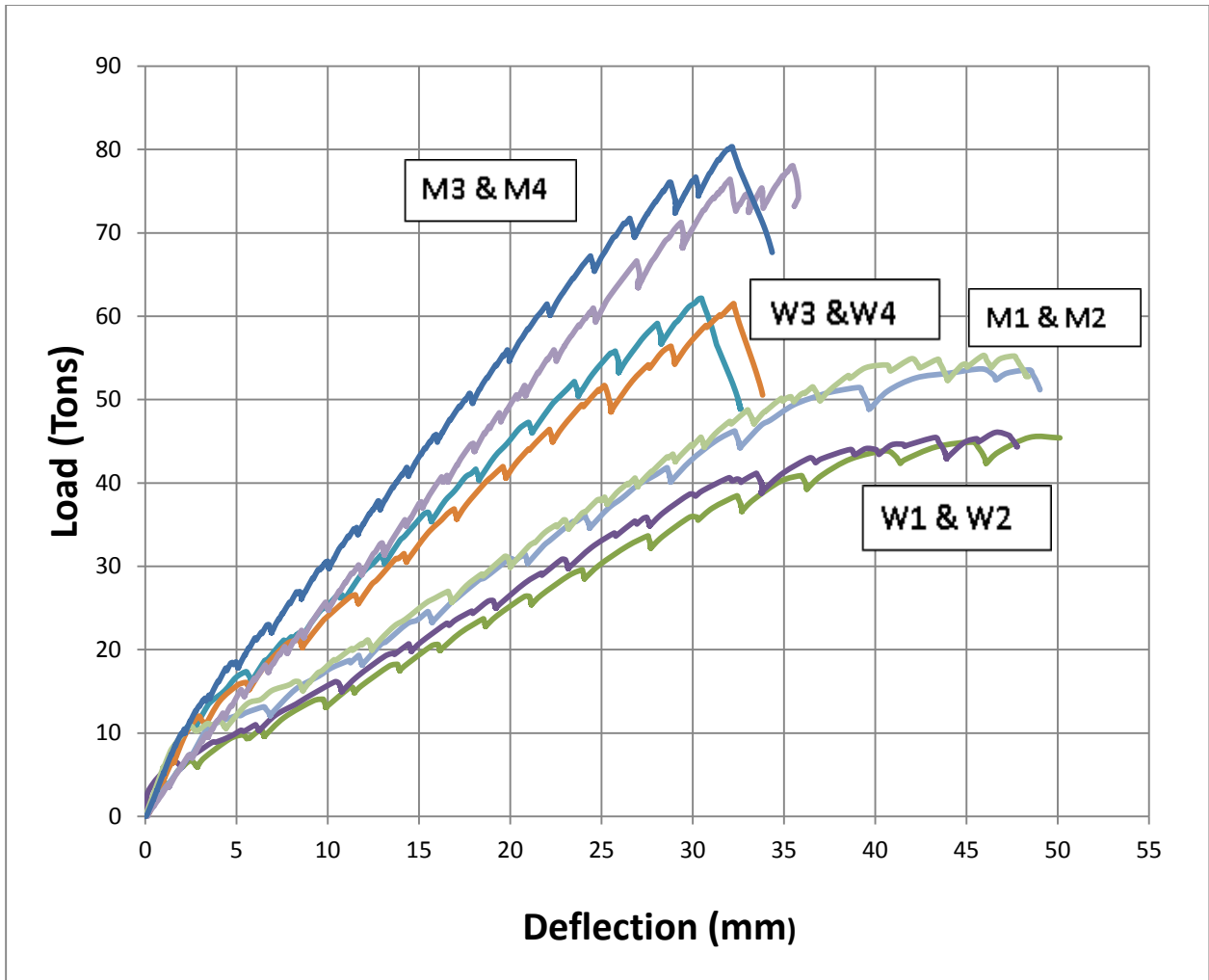


Fig. 4.37 Combined behaviors of all beams

Table 4.1 shows the summary of test results of all beams

Beam	ρ	Mn Theoretical k-ft	Mn Experimental k-ft	P Theoretical kips	P Experimental Kips	Remarks
W1	0.0136	131	150.45	43.45	50.14	Tension Controlled
W2	0.0136	131	152.05	43.45	50.69	Tension Controlled
W3	0.0276	197.53	195.37	67.33	66.67	Shear Compression Failure
W4	0.0276	197.53	196.95	67.33	67.22	Shear Compression Failure
M1	0.0127	165.53	182.45	54.79	60.61	Tension Controlled
M2	0.0127	165.53	179.25	54.79	59.51	Tension Controlled
M3	0.0259	255	252.07	86.96	85.95	Shear Compression Failure
M4	0.0259	255	258.39	86.96	88.16	Shear Compression Failure

Table 4.1 Summary of Test Results of All Beams

Chapter-5

CONCLUSIONS AND RECOMMENDATIONS

5.1 Behavior of Medium Reinforced Concrete Wide Beams

As mentioned earlier, specimens W1, W2, M1 and M2 were medium reinforced ($\rho=0.59\rho_b$ and $0.65\rho_b$). Moment capacity achieved was 15% and 16% more than the theoretical for W1 and W2 respectively while M1 and M1 achieved 10% and 8% increased moment capacity irrespective of the width of the beam. No considerable widening of shear cracks was observed. As the load was increased, flexure cracks became wider and penetrated into depth of the beam. Ultimate failure was recognized at deflections of 47-50mm when the load stopped increasing. These beams behaved in ductile manner through the failure. Theoretical deflections were calculated using second degree analysis given in ACI code. It was observed that the experimental deflections were greater than those calculated theoretically.

5.2 Behavior of Highly Reinforced Concrete Wide Beams

Specimens W3, W4, M3 and M4 were highly reinforced ($\rho=0.95\rho_b$). All beams were designed in a way that flexure failure would occur before shear failure. These beams just achieved their designed moment capacity. Shear cracks became wider with the load and penetrated into the compression zone causing shear-compression failure. No significant widening of flexure cracks was observed. Ultimate failure was recognized by a sharp sound and beams failed in a brittle manner. It was also noted that theoretical deflections were in good agreement with the experimental deflections. Shear cracks started at a distance equal to 1.5 times the effective depth of the beam measured from centre of the support. Inclination of shear cracks varied between 35-40 degrees.

5.3 Discussion

A reinforced concrete beam is always desired to fail in a tension controlled manner. Design calculations are made considering the strength and serviceability criteria. It is important to note that moment capacity of a beam varies linearly with the effective depth of the beam, while deflection is inversely proportional to the cube root of beam depth. Wide beams, because of small depths, have low relative stiffness and undergo large deflections. In this way use of wide beam in structural floor system may compromise one of the two criteria i.e. strength and serviceability. This study has shown that deflections can be controlled by providing high longitudinal reinforcement ratios. It was also evident that at high reinforcement ratios mode of failure changes from ductile to brittle manner.

Specimens W3, W4, M3 and M4 failed ultimately in shear-compression before achieving their designed flexural capacity indicating that shear mechanism is still not fully understood and ACI shear equations cannot be blindly applied to wide beams. Balanced failure is based on the balance reinforcement ratio calculated from the linear strain distribution across the depth of the beam and it is not directly related to shear strength. A beam reinforced under balanced conditions will start failing by yielding of tensile reinforcement rather by crushing of concrete in compression zone at ultimate loads. Shear strength is estimated using empirical equation given in ACI code. It is observed that the wide beams reinforced under balanced conditions may fail in shear at load less than that predicted by ACI equations. W3 and W4 failed in shear-compression at 25% less load than predicted by ACI shear equation. M3 and M4 also failed in shear-compression at 10% and 8% load less than that calculates from ACI equation respectively. Reduction in shear strength was more in case of W3 and W4. Doubling the reinforcement ratio for the same cross-section decreased the deflections by 40% at ultimate loads.

5.4 Conclusions

The following conclusions have been drawn from the study:

1. Flexural moment capacity of reinforced concrete wide beams may be estimated applying normal design procedures
2. At high longitudinal reinforcement ratios (ρ being closer to ρ_b), experimental moment capacities are just equal to theoretical moment capacities but the wide beam may fail at a load less than that predicted by ACI shear equation.
3. Deflection can be controlled by increasing the longitudinal reinforcement ratio but the mode of failure may change from tension controlled to shear compression even under balance reinforcement provisions.
4. Wide beams can be shear critical while meeting high flexural demands hence should not be exempted from the minimum shear reinforcement provisions given in ACI-318-14.

5.5 Recommendations

ACI Shear equation $2\sqrt{f'_c} * b * d$, developed on the basis of 194 tests having an average size of 194 mm (7.6 in.) wide by 340 mm (13.4 in.) deep, was intended to be a conservative estimate of the average shear stress at which diagonal shear cracks form. In the absence of shear reinforcement to control these cracks, this was believed to be an appropriate estimate of the shear strength of the member. Unfortunately, it was not identified at the time that wide beam may fail at a load less than that predicted by aforementioned equation while meeting high flexural demands. The commentary in Section R11.5.6.1 of ACI 318-05 discussing the exceptions notes that wide beams and slabs are “excluded from the minimum shear reinforcement requirement because there is a possibility of load sharing between weak and strong areas.” This assumption becomes questionable when a nearly uniform shear demand exists across the full width of a one-way spanning member. In view of all above it is strongly recommended that shear behavior of reinforced concrete wide beams at high reinforcement ratios without web reinforcement needs to be studied and understood.

APPENDIX I

APPENDIX I

W1

Load (Tons)	Mid Deflection (mm)	Quarter Deflection (mm)
0	0	0
3.79	1.31	1.21
3.77	1.31	1.21
3.76	1.31	1.21
6.40	2.26	1.99
6.25	2.74	2.35
6.11	2.81	2.38
6.07	2.82	2.39
6.03	2.84	2.39
6.01	2.85	2.40
5.98	2.86	2.40
9.31	4.63	3.73
10.01	6.46	4.99
9.88	6.48	5.01
9.81	6.49	5.02
9.77	6.50	5.03
9.73	6.51	5.04
9.71	6.51	5.04
9.68	6.51	5.04
9.67	6.52	5.05
9.65	6.52	5.05
9.61	6.53	5.05
13.56	9.84	7.49
13.33	9.88	7.50

Load (Tons)	Mid Deflection (mm)	Quarter Deflection (mm)
13.25	9.89	7.51
13.21	9.89	7.51
13.17	9.89	7.52
13.14	9.90	7.52
13.12	9.90	7.52
13.10	9.90	7.52
13.08	9.91	7.53
13.07	9.91	7.53
15.14	11.43	8.64
15.02	11.44	8.66
14.95	11.45	8.67
14.90	11.46	8.67
14.87	11.47	8.67
17.85	13.89	10.44
17.66	13.92	10.47
17.57	13.93	10.48
17.51	13.94	10.48
17.47	13.94	10.49
20.19	16.12	12.08
20.06	16.13	12.09
19.99	16.14	12.10
19.94	16.14	12.10
19.90	16.14	12.11
23.09	18.62	13.92
22.94	18.63	13.93
22.86	18.64	13.94
22.80	18.64	13.94

Load (Tons)	Mid Deflection (mm)	Quarter Deflection (mm)
25.98	21.11	15.74
25.75	21.13	15.76
25.62	21.15	15.77
25.54	21.15	15.77
25.48	21.16	15.78
25.43	21.16	15.78
29.38	23.97	17.77
28.86	24.04	17.84
28.71	24.06	17.86
28.62	24.06	17.87
28.55	24.07	17.88
33.44	27.57	20.40
32.76	27.67	20.50
32.59	27.69	20.52
32.48	27.69	20.53
32.40	27.70	20.54
32.33	27.70	20.54
37.75	32.57	24.10
37.26	32.65	24.18
37.07	32.68	24.20
36.95	32.68	24.21
36.84	32.69	24.22
40.89	35.94	26.29
39.81	36.21	26.45
39.59	36.24	26.46
39.44	36.25	26.47
39.32	36.25	26.47

Load (Tons)	Mid Deflection (mm)	Quarter Deflection (mm)
42.62	41.30	28.02
43.06	45.98	28.11
42.71	46.04	28.11
42.52	46.07	28.11
42.35	46.08	28.12

W2

Load (Tons)	Mid Deflection (mm)	Quarter Deflection (mm)
0	0	0
5.92	1.98	1.77
5.89	1.99	1.78
10.50	6.18	4.91
10.36	6.22	4.93
10.30	6.23	4.94
15.60	10.68	8.25
15.43	10.71	8.27
15.35	10.73	8.28
15.30	10.73	8.29
15.26	10.74	8.29
15.22	10.74	8.30
15.20	10.75	8.30
15.17	10.75	8.30
15.15	10.75	8.30
15.13	10.75	8.30

Load (Tons)	Mid Deflection (mm)	Quarter Deflection (mm)
15.11	10.76	8.31
15.10	10.76	8.31
15.08	10.76	8.31
15.07	10.76	8.31
15.06	10.76	8.31
15.05	10.76	8.31
15.04	10.77	8.31
15.03	10.77	8.31
15.02	10.77	8.32
15.01	10.77	8.32
15.00	10.77	8.32
14.99	10.77	8.32
20.15	14.54	11.13
19.99	14.56	11.14
19.91	14.57	11.15
19.86	14.58	11.15
19.81	14.59	11.16
25.53	19.13	14.42
25.30	19.17	14.44
25.20	19.19	14.45
25.13	19.20	14.46
25.08	19.20	14.46
25.04	19.21	14.46
25.00	19.21	14.47
24.97	19.22	14.47
30.33	23.10	17.35
30.09	23.14	17.38

Load (Tons)	Mid Deflection (mm)	Quarter Deflection (mm)
29.97	23.16	17.39
29.87	23.17	17.39
29.80	23.17	17.39
29.75	23.18	17.40
35.74	27.28	20.47
35.32	27.58	20.69
35.15	27.61	20.70
35.06	27.62	20.71
34.98	27.63	20.72
34.92	27.64	20.72
34.87	27.64	20.73
40.08	32.65	24.33
40.24	33.72	25.23
40.02	33.76	25.26
39.89	33.78	25.27
39.80	33.79	25.28
39.72	33.80	25.29
39.65	33.81	25.30
39.59	33.82	25.30
39.55	33.82	25.30
39.49	33.82	25.30
39.43	33.82	25.30
39.38	33.81	25.30
39.34	33.81	25.30
39.30	33.81	25.30
39.26	33.80	25.30
39.22	33.80	25.30

Load (Tons)	Mid Deflection (mm)	Quarter Deflection (mm)
39.19	33.80	25.30
39.16	33.79	25.30
39.13	33.79	25.30
39.10	33.79	25.29
39.07	33.79	25.29
39.04	33.78	25.29
39.02	33.78	25.29
39.00	33.78	25.29
38.98	33.78	25.29
38.96	33.78	25.29
38.94	33.78	25.29
38.92	33.77	25.28
38.90	33.77	25.28
38.88	33.77	25.28
38.87	33.77	25.28
38.85	33.77	25.28
38.84	33.77	25.28
38.83	33.77	25.28
38.81	33.77	25.28
44.31	43.67	31.10
43.74	43.80	31.12
43.54	43.84	31.12
43.40	43.87	31.12
43.30	43.88	31.12
43.22	43.90	31.13
43.15	43.91	31.13
43.08	43.91	31.13

Load (Tons)	Mid Deflection (mm)	Quarter Deflection (mm)
43.01	43.91	31.13
42.94	43.91	31.13
45.07	47.57	32.41
44.58	47.72	32.43
44.39	47.76	32.43

W3

Load (Tons)	Mid Deflection (mm)	Quarter Deflection (mm)
0	0	0
6.47	1.54	1.09
6.49	1.55	1.10
6.50	1.56	1.11
6.52	1.57	1.11
6.53	1.57	1.12
6.54	1.58	1.12
6.55	1.58	1.12
11.19	3.22	2.38
11.06	3.25	2.40
10.99	3.27	2.42
10.95	3.28	2.42
10.91	3.28	2.43
15.76	5.60	4.36

Load (Tons)	Mid Deflection (mm)	Quarter Deflection (mm)
15.46	5.67	4.42
15.36	5.69	4.43
15.29	5.69	4.44
15.25	5.70	4.45
20.95	8.48	6.69
20.59	8.56	6.75
20.47	8.58	6.77
20.39	8.60	6.77
20.34	8.61	6.78
20.29	8.61	6.79
20.25	8.62	6.79
25.95	11.62	9.15
25.79	11.64	9.17
25.69	11.66	9.18
25.62	11.67	9.19
25.57	11.67	9.19
25.53	11.68	9.19
31.29	14.21	11.25
30.95	14.26	11.30
30.82	14.28	11.31
30.73	14.29	11.32
30.66	14.30	11.33
30.60	14.30	11.33
30.55	14.31	11.33
30.51	14.31	11.34
36.47	16.98	13.52

Load (Tons)	Mid Deflection (mm)	Quarter Deflection (mm)
36.19	17.03	13.55
36.05	17.04	13.57
35.96	17.06	13.57
35.89	17.06	13.58
35.82	17.07	13.58
35.77	17.07	13.58
35.71	17.07	13.59
40.70	18.96	15.09
41.29	19.70	15.69
41.10	19.73	15.71
40.97	19.74	15.72
40.88	19.75	15.73
40.79	19.76	15.73
40.72	19.76	15.74
40.65	19.76	15.74
40.60	19.76	15.74
45.92	22.23	17.64
45.61	22.27	17.68
45.46	22.29	17.70
45.33	22.31	17.71
45.24	22.31	17.72
45.15	22.32	17.72
45.07	22.32	17.72
45.00	22.32	17.72
44.94	22.32	17.73
49.42	24.11	19.17

Load (Tons)	Mid Deflection (mm)	Quarter Deflection (mm)
50.61	25.35	20.27
49.97	25.42	20.41
49.62	25.46	20.49
49.44	25.48	20.53
49.32	25.50	20.55
49.22	25.50	20.56
49.14	25.51	20.57
49.07	25.51	20.57
48.98	25.51	20.58
48.91	25.51	20.58
48.84	25.51	20.58
48.77	25.51	20.58
48.71	25.51	20.57
48.65	25.52	20.57
48.60	25.52	20.57
48.56	25.52	20.57
48.52	25.52	20.57
55.69	28.90	23.42
55.26	28.96	23.48
55.03	28.99	23.50
54.85	29.00	23.51
54.70	29.01	23.52
54.57	29.01	23.53
54.46	29.02	23.53
54.35	29.02	23.53
54.24	29.01	23.53

W4

Load (Tons)	Mid Deflection (mm)	Quarter Deflection (mm)
0	0	0
6.76	1.41	1.41
6.73	1.41	1.41
6.71	1.41	1.41
6.70	1.41	1.41
11.12	2.71	2.71
10.95	2.75	2.75
10.88	2.76	2.76
10.83	2.77	2.77
10.79	2.77	2.77
16.91	5.67	5.67
16.54	5.77	5.77
16.43	5.79	5.79
16.35	5.81	5.81
16.30	5.82	5.82
16.25	5.83	5.83
21.28	8.06	8.06
21.56	8.48	8.48
21.42	8.50	8.50
21.34	8.51	8.51
21.28	8.52	8.52
26.42	10.82	10.82
26.16	10.86	10.86
26.05	10.88	10.88

Load (Tons)	Mid Deflection (mm)	Quarter Deflection (mm)
25.97	10.89	10.89
31.27	12.97	12.97
30.73	13.07	13.07
30.58	13.10	13.10
30.48	13.11	13.11
30.40	13.12	13.12
30.33	13.12	13.12
36.20	15.57	15.57
35.85	15.64	15.64
35.70	15.66	15.66
35.59	15.67	15.67
35.50	15.67	15.67
35.42	15.68	15.68
35.36	15.68	15.68
41.06	18.22	18.22
40.82	18.26	18.26
40.69	18.28	18.28
40.58	18.29	18.29
40.47	18.29	18.29
40.39	18.29	18.29
47.17	21.03	21.03
46.54	21.14	21.14
46.34	21.17	21.17
46.20	21.19	21.19
46.08	21.20	21.20
52.01	23.53	23.53
51.27	23.66	23.66

Load (Tons)	Mid Deflection (mm)	Quarter Deflection (mm)
51.01	23.70	23.70
50.84	23.72	23.72
50.70	23.73	23.73
50.58	23.73	23.73
50.46	23.73	23.73
55.34	25.83	25.83
54.92	25.89	25.89
54.61	25.93	25.93
54.41	25.95	25.95
54.23	25.96	25.96
54.09	25.96	25.96
53.95	25.95	25.95
53.81	25.95	25.95
53.70	25.95	25.95
53.59	25.95	25.95
53.50	25.95	25.95
53.41	25.94	25.94
53.34	25.94	25.94
53.27	25.94	25.94
58.36	28.16	28.16
57.97	28.22	28.22
57.74	28.25	28.25
57.56	28.27	28.27
57.40	28.28	28.28
57.27	28.28	28.28
57.12	28.28	28.28
56.99	28.28	28.28

Load (Tons)	Mid Deflection (mm)	Quarter Deflection (mm)
56.87	28.28	28.28
56.77	28.28	28.28
56.67	28.27	28.27
60.73	30.71	30.71
58.28	31.10	31.10
57.48	31.20	31.20
50.73	32.39	32.39
50.16	32.47	32.47
49.83	32.50	32.50
49.58	32.53	32.53
49.38	32.56	32.56
49.20	32.58	32.58
49.06	32.59	32.59
48.95	32.61	32.61

M1

Load (Tons)	Mid Deflection (mm)	Quarter Deflection (mm)
0	0	0
7.17	2.48	1.85
7.14	2.49	1.85
7.13	2.49	1.85
7.11	2.49	1.85
7.10	2.49	1.86
7.09	2.49	1.86
13.14	6.48	1.86
12.42	6.77	2.79
12.32	6.80	5.03
12.25	6.82	5.07
12.21	6.83	5.08
12.17	6.84	5.09
12.15	6.84	5.10
12.12	6.85	5.11
12.10	6.85	5.11
17.82	10.20	5.12
18.81	11.79	5.12
18.42	11.85	5.12
18.34	11.86	8.82
18.29	11.87	8.88
18.26	11.87	8.98
18.23	11.88	8.99
18.20	11.88	9.00
18.17	11.88	9.00

Load (Tons)	Mid Deflection (mm)	Quarter Deflection (mm)
23.91	15.64	9.01
23.66	15.69	9.01
23.56	15.71	9.01
23.47	15.72	10.90
23.41	15.73	11.94
23.36	15.73	11.97
23.33	15.74	11.98
23.29	15.72	11.98
23.26	15.72	11.99
28.34	18.27	11.99
31.03	20.88	12.00
30.82	20.91	12.00
30.70	20.93	12.00
30.61	20.94	12.00
30.55	20.94	14.19
30.49	20.95	16.01
30.43	20.95	16.04
30.38	20.96	16.06
36.10	24.09	16.07
35.35	24.26	16.07
35.14	24.30	16.08
35.03	24.32	16.08
34.95	24.33	16.09
34.88	24.34	16.09
34.83	24.34	18.02
34.78	24.35	18.67
34.74	24.35	18.72

Load (Tons)	Mid Deflection (mm)	Quarter Deflection (mm)
34.70	24.35	18.74
34.66	24.35	18.75
34.63	24.36	18.75
34.60	24.36	18.76
41.37	28.66	18.76
40.93	28.73	18.77
40.75	28.75	18.77
40.64	28.76	18.77
40.55	28.77	18.77
40.48	28.78	18.78
40.42	28.78	18.78
40.36	28.78	18.78
40.31	28.79	22.10
40.27	28.79	22.15
40.23	28.79	22.17
40.19	28.79	22.18
40.15	28.79	22.19
40.11	28.79	22.20
45.46	32.44	22.20
45.12	32.50	22.21
44.95	32.52	22.21
44.83	32.54	22.22
44.74	32.55	22.22
44.66	32.55	22.22
44.60	32.56	22.22
44.54	32.57	22.22
44.48	32.57	22.22

Load (Tons)	Mid Deflection (mm)	Quarter Deflection (mm)
44.44	32.57	23.08
44.39	32.57	25.04
44.34	32.57	25.07
44.29	32.57	25.08
44.25	32.57	25.10
49.38	35.55	25.11
49.92	39.50	25.11
49.55	39.57	25.12
49.34	39.60	25.12
49.20	39.62	25.13
49.09	39.64	25.13
49.00	39.65	25.14
48.93	39.66	25.14
48.86	39.66	25.14
52.78	48.69	25.14
51.78	48.92	25.14
51.46	48.98	25.14
51.27	49.01	30.31

M2

Load (Tons)	Mid Deflection (mm)	Quarter Deflection (mm)
0	0	0
5.83	1.00	0.84
11.07	4.26	1.83
10.83	4.34	2.95
10.69	4.39	2.98
10.62	4.41	2.99
10.56	4.42	3.00
15.55	8.56	3.01
15.39	8.59	5.68
15.31	8.61	5.70
15.25	8.61	5.71
15.20	8.62	5.71
15.17	8.63	5.71
15.14	8.63	5.72
15.11	8.63	5.72
15.09	8.63	5.72
20.61	12.33	5.72
20.35	12.37	5.73
20.06	12.41	8.24
20.01	12.41	8.27
19.98	12.42	8.29
26.36	16.72	8.29
26.10	16.76	8.29
25.98	16.78	9.13
25.86	16.79	11.18

Load (Tons)	Mid Deflection (mm)	Quarter Deflection (mm)
25.78	16.79	11.21
25.72	16.79	11.22
27.67	17.59	11.22
30.56	19.96	11.22
30.38	19.99	11.22
30.27	20.00	11.22
30.18	20.01	13.32
30.10	20.01	13.35
30.04	20.01	13.36
29.99	20.01	13.37
29.94	20.01	13.37
35.57	23.02	13.37
35.00	23.13	13.37
34.83	23.16	13.37
34.72	23.17	13.37
34.63	23.18	14.05
34.57	23.19	15.46
34.51	23.20	15.48
38.18	25.19	15.49
37.83	25.26	15.50
37.69	25.28	15.51
37.58	25.30	15.51
37.50	25.31	15.52
39.89	26.45	16.87
40.19	26.91	16.93
40.02	26.94	16.95
39.91	26.95	16.96

Load (Tons)	Mid Deflection (mm)	Quarter Deflection (mm)
39.82	26.96	16.97
39.75	26.97	16.97
39.68	26.97	18.01
39.62	26.98	18.04
39.57	26.98	18.06
43.16	28.96	18.07
42.91	29.00	18.07
42.78	29.03	18.08
42.67	29.04	18.08
42.58	29.05	18.08
45.50	30.44	18.09
44.96	30.55	18.60
44.78	30.58	19.43
44.65	30.60	19.45
44.56	30.61	19.47
44.48	30.62	19.47
44.41	30.63	19.48
44.35	30.63	20.11
48.10	33.17	20.51
47.61	33.28	20.54
47.40	33.32	20.55
47.26	33.34	20.56
47.16	33.35	20.57
50.08	35.45	20.58
50.63	36.83	20.58
50.24	36.92	20.58
50.03	36.96	22.28

Load (Tons)	Mid Deflection (mm)	Quarter Deflection (mm)
49.89	36.98	22.38
53.84	43.68	22.41
52.92	43.86	22.42
52.60	43.92	22.44
52.40	43.95	22.44
52.32	43.99	23.91
53.99	47.99	24.79
53.40	48.15	24.84
53.13	48.22	24.86
52.96	48.26	24.88
52.81	48.28	29.03

M3

Load (Tons)	Mid Deflection (mm)	Quarter Deflection (mm)
0	0	0
3.56	1.28	1.07
3.55	1.29	1.07
3.53	1.29	1.07
3.52	1.29	1.07
3.52	1.29	1.07
7.20	2.53	2.05
7.12	2.55	2.06
6.97	2.58	2.08
9.70	3.41	2.68
9.59	3.43	2.69
9.54	3.43	2.69
9.51	3.44	2.70
12.26	4.28	3.27
12.02	4.32	3.29
11.94	4.34	3.30
11.89	4.35	3.31
11.85	4.35	3.31
14.90	5.33	3.98
14.62	5.39	4.02
14.52	5.41	4.03
14.46	5.42	4.04
14.42	5.43	4.04
17.65	6.68	4.90
17.46	6.72	4.92
17.37	6.74	4.93

Load (Tons)	Mid Deflection (mm)	Quarter Deflection (mm)
17.31	6.75	4.94
19.90	7.73	5.62
19.74	7.76	5.64
19.64	7.78	5.65
19.58	7.79	5.65
21.99	8.63	6.24
21.81	8.66	6.26
21.71	8.67	6.27
21.64	8.68	6.27
21.59	8.68	6.28
21.55	8.69	6.28
21.51	8.69	6.28
21.48	8.70	6.29
21.45	8.70	6.29
25.20	9.97	7.19
25.02	10.00	7.21
24.92	10.01	7.22
24.86	10.02	7.22
24.79	10.02	7.23
24.74	10.03	7.23
29.63	11.79	8.44
29.38	11.83	8.46
29.25	11.84	8.47
29.16	11.85	8.48
29.08	11.85	8.48
29.02	11.85	8.48
28.97	11.86	8.48

Load (Tons)	Mid Deflection (mm)	Quarter Deflection (mm)
32.45	13.03	9.28
32.26	13.06	9.30
32.14	13.07	9.31
32.05	13.07	9.31
31.97	13.08	9.31
31.91	13.08	9.32
31.86	13.09	9.32
31.81	13.08	9.32
31.76	13.08	9.32
31.72	13.08	9.32
31.68	13.09	9.32
31.65	13.09	9.32
31.63	13.09	9.32
31.60	13.09	9.32
31.58	13.09	9.32
31.56	13.09	9.32
31.54	13.09	9.32
31.52	13.09	9.32
31.51	13.09	9.32
31.49	13.10	9.32
31.48	13.10	9.33
31.47	13.10	9.33
31.46	13.10	9.33
31.44	13.10	9.33
31.43	13.11	9.33
31.42	13.11	9.33
31.41	13.11	9.33

Load (Tons)	Mid Deflection (mm)	Quarter Deflection (mm)
31.40	13.11	9.33
35.33	14.27	10.12
35.12	14.29	10.14
35.01	14.30	10.14
34.92	14.30	10.15
34.85	14.30	10.15
37.67	15.13	10.70
37.37	15.17	10.73
37.23	15.19	10.74
37.13	15.19	10.75
37.05	15.19	10.75
40.54	16.26	11.47
40.16	16.31	11.50
40.76	16.55	11.67
40.60	16.57	11.68
40.47	16.57	11.69
40.37	16.57	11.69
40.28	16.57	11.69
40.21	16.57	11.69
40.14	16.57	11.69
44.69	17.98	12.65
44.31	18.02	12.68

Load (Tons)	Mid Deflection (mm)	Quarter Deflection (mm)
0	0	0
5.16	1.01	0.73
5.14	1.01	0.73
10.36	2.14	1.49
10.15	2.17	1.51
10.06	2.18	1.51
12.90	2.84	1.96
13.87	3.31	2.27
14.41	3.51	2.40
14.28	3.53	2.41
14.21	3.53	2.41
14.15	3.54	2.41
18.37	5.01	3.34
18.11	5.06	3.38
18.00	5.07	3.39
17.92	5.09	3.40
17.86	5.09	3.40
20.22	5.70	3.79
22.52	6.86	4.54
22.33	6.89	4.56
22.23	6.90	4.57
22.23	6.91	4.58
22.18	6.91	4.58
22.14	6.91	4.58
22.11	6.92	4.59
22.08	6.92	4.59
22.05	6.92	4.59

Load (Tons)	Mid Deflection (mm)	Quarter Deflection (mm)
26.92	8.28	5.46
26.57	8.53	5.64
26.42	8.55	5.65
26.30	8.55	5.66
26.21	8.55	5.66
26.14	8.56	5.66
26.21	8.58	5.68
30.50	10.01	6.60
30.22	10.04	6.63
30.09	10.06	6.64
29.96	10.06	6.65
29.86	10.06	6.65
29.80	10.06	6.65
29.76	10.06	6.65
33.45	11.14	7.33
34.31	11.63	7.65
34.14	11.65	7.66
34.00	11.65	7.67
33.87	11.65	7.67
37.82	12.80	8.40
37.36	12.86	8.44
37.18	12.87	8.45
37.01	12.87	8.45
36.89	12.87	8.45
36.81	12.87	8.45
41.53	14.39	9.43
41.23	14.42	9.46

Load (Tons)	Mid Deflection (mm)	Quarter Deflection (mm)
41.04	14.42	9.46
40.85	14.42	9.46
44.85	15.59	10.21
45.40	15.99	10.48
45.17	16.01	10.50
44.94	16.01	10.50
49.98	17.55	11.50
50.23	17.89	11.74
50.04	17.92	11.77
49.89	17.93	11.78
49.74	17.94	11.78
49.58	17.93	11.78
55.82	19.87	13.03
55.28	19.94	13.10
55.02	19.95	13.11
54.73	19.95	13.11
56.97	20.50	13.46
60.75	22.11	14.51
60.47	22.15	14.55
60.28	22.17	14.57
60.14	22.19	14.58
66.63	24.48	16.06
66.14	24.54	16.11
65.87	24.58	16.13
65.66	24.60	16.15
65.48	24.61	16.15
71.19	26.63	17.42

Load (Tons)	Mid Deflection (mm)	Quarter Deflection (mm)
70.35	26.74	17.47
70.06	26.77	17.50
69.84	26.79	17.52
69.66	26.80	17.52
69.48	26.81	17.53
75.64	28.85	18.88
74.77	28.95	19.03
74.17	29.01	19.16
73.81	29.05	19.23
73.56	29.07	19.26
73.32	29.07	19.28
73.10	29.07	19.28
72.90	29.06	19.29
72.73	29.05	19.29
72.58	29.05	19.29
72.45	29.04	19.29
76.15	29.97	19.90
76.13	30.23	20.11
75.76	30.27	20.18
75.45	30.29	20.23
75.18	30.31	20.27

REFERENCES

1. ASCE-ACI Committee 426: The Shear Strength of Reinforced Concrete Members. *ASCE Journal of Structural Division*, 1973, 99, No. 6, pp. 1091 –1187.
2. Kani, G. N. J., “How Safe Are Our Large Concrete Beams?,” *ACI JOURNAL Proceedings*, V. 64, No. 3, Mar. 1967, pp. 128-141.
3. Kuchma, D.; Végh, P.; Simionopoulos, K.; Stanik, B.; Collins, M. P., “The Influence of Concrete Strength, Distribution of Longitudinal Reinforcement and Member Size on the Shear Strength of Reinforced Concrete Beams,” *CEB Bulletin No. 237*, 21 pp.
4. Bazant, Z. P., and Kazemi, M. T., “Size Effect on Diagonal Shear Failure of Beams without Stirrups,” *ACI Structural Journal*, V. 88, No. 3, May-June 1991, pp. 268-276.
5. Shioya, T.; Iguro, M. Nojirr, Y., Akiyama, H.; and Okada, T., “Shear Strength of Large Reinforced Concrete Beams,” *Fracture Mechanics: Application to Concrete*, SP-118, V. C. Li and Z. P. Bazant, eds., American Concrete Institute, Farmington Hills, Mich., 1989, pp. 259-279.
6. Shioya, T., “Shear Properties of Large Reinforced Concrete Member,” Special Report of Institute of Technology, Shimizu Corp., No. 25, Feb. 1989, 198 pp.
7. ACI Committee 318, “Building Code Requirements for Structural Concrete (ACI 318-95) and Commentary,” American Concrete Institute, Farmington Hills, MI, 1995, 369 pp.
8. ACI-ASCE Committee 326, “Shear and Diagonal Tension,” *ACI JOURNAL*, Proceedings V. 59, No. 1-3, Jan.-Mar. 1962, pp. 1-30, 277-344, and 352-396.
9. Popov, E. P.; Cohen, J. M.; Thomas, K. K.; Kasai, k., “Behavior of Interior Narrow and Wide Beams,” *ACI Structural Journal*, V. 89, No. 6, November-December 1992, pp.607-616.
10. Collins, M. P., and Kuchma, D., “How Safe Are Our Large, Lightly Reinforced, Concrete Beams, Slabs, and Footings” *ACI Structural Journal*, V. 96, No. 4, July-Aug. 1999, pp. 482-490.
11. Tompos, E. J., and Frosch, R. J., “Influence of Beam Size, Longitudinal Reinforcement, and Stirrup Effectiveness on Concrete Shear Strength,” *ACI Structural Journal*, V. 99, No. 5, Sept.-Oct. 2002, pp. 559-567.
12. Lubell, A.; Sherwood, T.; Bentz, E.; and Collins, M. P., “Safe Shear Design of Large Wide Beams,” *Concrete International*, V. 26, No. 1, Jan. 2004, pp. 66-78
13. Sherwood, E. G.; Lubell, A. S.; Bentz, E. C.; and Collins, M. P., “One Way Shear Strength of Thick Slabs and Wide Beams,” *ACI Structural Journal*, V. 103, No. 6, Nov.-Dec. 2006, pp. 794-802.
14. Lubell, A. S.; Bentz, E. C.; and Collins, M. P., “Influence of Longitudinal Reinforcement on One-Way Shear in Slabs and Wide Beams,” *Journal of Structural Engineering*, ASCE, V. 135, No. 1, 2009, pp. 78-87. doi: 10.1061/(ASCE)0733-9445(2009)135:1(78)

15. Serna-Ros, P.; Fernandez-Prada, M. A.; Miguel-Sosa, P.; and Debb, O. A. R., "Influence of Stirrup Distribution and Support Width on the Shear Strength of Reinforced Concrete Wide Beams," *Magazine of Concrete Research*, V. 54, No. 3, 2002, pp. 181-191. doi: 10.1680/mac.2002.54.3.181
16. Lubell, A. S.; Bentz, E. C.; and Collins, M. P., "Shear Reinforcement Spacing in Wide Members," *ACI Structural Journal*, V. 106, No. 2, Mar.-Apr. 2009, pp. 205-214
17. Hanfey, M. M.; Mohammad, H. M.; and Yehia, N. A.B., "On the Contribution of Shear Reinforcement in Shear Strength of Shallow Wide Beams" *Life Science Journal*, 2012;9(3):484-498
18. Lofty, E. M.; Mohamadien, H. A.; and Hassan, H. M., "Effect of Web Reinforcement on Shear Strength of Shallow Wide Beams" *international Journal of Engineering and Technical Research (LJETR)* ISSN: 2321-0869, Volume-2, Issue-11, November 2014, pp. 98-107
19. Lantsought, E. O. L.; Veen, C. V. D.; Boer, A. D.; and Walrawven, J. C., "Influence of Width on Shear Capacity of Reinforced Concrete Members" *ACI Structural Journal*, V. 111, No. 6, November-December 2014. MS No. S-2013-258, doi: 10.14359/51687107. pp. 1441-1450
20. Yasouj, S. E.; Marsono, A. K.; Abdullah, R.; and Moghadasi, M., "Wide Beam Shear Behavior with Diverse Type of Reinforcement" *ACI Structural Journal*, V. 111, No. 1-6, January-December 2014. MS No. S-2013-360.R4, doi: 10.14359/51687299. Pp. 1-10
21. Elrakib, T.M.; and Said, M., " Enhancement of Shear Strength and Ductility for Reinforced Concrete Wide Beams Due to Web Reinforcement " *Housing and Building National Research Center Journal*, (2013) 9, 235-242
22. Conforti, A.; Minelli, F.; and Plizzari, G.A., "Wide-shallow beams with and without steel fibers: A peculiar behavior in shear and flexure" Department of Civil Engineering, Architecture, Land, Environment and Mathematics, University of Brescia, Italy *Composites: Part B* 51 (2013) 282–290
23. Ahmed, A.M.; and Shuraim, A.M., "Transverse Stirrup Configuration in RC Wide Shallow Beams Supported on Narrow Columns" *Journal of Structural Engineering*, Vol. 138, No. 3, March 1, 2012. ©ASCE, ISSN 0733-9445/2012/3-416 –424